Btn3 is a negative regulator of Btn2-mediated endosomal protein trafficking and prion curing in yeast

Vydehi Kanneganti, Rachel Kama, and Jeffrey E. Gerst
Department of Molecular Genetics, Weizmann Institute of Science, Rehovot 76100, Israel

ABSTRACT **Yeast Btn2 facilitates the retrieval of specific proteins from late endosomes (LEs) to the Golgi, a process that may be adversely affected in Batten disease patients. We isolated the putative yeast orthologue of a human complex I deficiency gene, designated here as *BTN3*, as encoding a Btn2-interacting protein and negative regulator. First, yeast overexpressing *BTN3* phenocopy the deletion of *BTN2* and mislocalize certain *trans*-Golgi proteins, like Kex2 and Yif1, to the LE and vacuole, respectively. In contrast, the deletion of *BTN3* results in a tighter pattern of protein localization to the Golgi. Second, *BTN3* overexpression alters Btn2 localization from the IPOD compartment, which correlates with a sharp reduction in Btn2-mediated [URE3] prion curing. Third, Btn3 and the Snc1 v-SNARE compete for the same binding domain on Btn2, and this competition controls Btn2 localization and function. The inhibitory effects upon protein retrieval and prion curing suggest that Btn3 sequesters Btn2 away from its substrates, thus down-regulating protein trafficking and aggregation. Therefore Btn3 is a novel negative regulator of intracellular protein sorting, which may be of importance in the onset of complex I deficiency and Batten disease in humans.**

Monitoring Editor
Sandra K. Lemmon
University of Miami

Received: Nov 4, 2010
Revised: Mar 9, 2011
Accepted: Mar 10, 2011

INTRODUCTION

Neuronal ceroid lipofuscinoses (NCLs) constitute a family of mammalian autosomal recessive disorders that lead to progressive neurodegeneration and early death. These diseases are typified by the abnormal accumulation of autofluorescent storage material in the lysosome, followed by subsequent neuron loss, and result from mutations in genes encoding either lysosomal enzymes or transmembranal proteins of unknown function (e.g., *CLN1–9*) (Mole *et al.*, 2005; Kyttala *et al.*, 2006; Rakheja *et al.*, 2008; Getty and Pearce, 2011).

Juvenile-onset NCL or Batten disease constitutes the principal NCL disorder and is caused by mutations in *CLN3*, a gene that encodes a multipass transmembrane domain–containing protein that has been shown to localize to lysosomes, endosomes, synaptosomes, and the cell membrane (Katz *et al.*, 1997; Jarvela *et al.*, 1998, 1999; Kremmidiotis *et al.*, 1999; Haskell *et al.*, 2000; Persaud-Sawin *et al.*, 2004). Yeast has been used as a model for Batten disease because they contain a *CLN3* orthologue, named *BTN1* (Pearce and Sherman, 1997; Croopnick *et al.*, 1998). Importantly, the deletion of *BTN1* leads to defects in vacuolar pH homeostasis and amino acid uptake to the vacuole, and is typified by the up-regulation of *BTN2*, a gene possibly involved in cellular adaptation to the loss of Btn1 (Pearce *et al.*, 1999; Chattopadhyay *et al.*, 2000; Chattopadhyay and Pearce, 2002).

Earlier work on *BTN2*, which encodes a Hook orthologue involved in endosomal processes in mammalian cells (Walenta *et al.*, 2001; Richardson *et al.*, 2004) and *Drosophila* (Kramer and Phistry, 1996; Sunio *et al.*, 1999), demonstrated that it physically interacts with Golgi, endosome, and plasma membrane (PM) proteins (e.g.,Yif1, Rhb1, and Ist2, respectively) and that the deletion of *BTN2* results in their altered localization (Chattopadhyay and Pearce, 2002; Chattopadhyay *et al.*, 2003; Kim *et al.*, 2005). In addition, the overexpression of *BTN2* led to decreased arginine uptake (Chattopadhyay and Pearce, 2002), although connection between these different phenotypes remains obscure. We identified *BTN2* as a soluble *N*-ethylmaleimide-sensitive fusion protein attachment protein receptor (SNARE)- and retromer-interacting protein that is directly involved in the recycling of cargo proteins from late endosomes (LEs)

This article was published online ahead of print in MBoC in Press (http://www.molbiolcell.org/cgi/doi/10.1091/mbc.E10-11-0878) on March 25, 2011.

Address correspondence to: Jeffrey E. Gerst (jeffrey.gerst@weizmann.ac.il).

Abbreviations used: GFP, green fluorescent protein; IP, immunoprecipitation; IPOD, insoluble protein deposit compartment; LE, late endosome; MVB, multivesicular body; SNARE, soluble *N*-ethylmaleimide-sensitive fusion protein attachment protein receptor; VPS, vacuolar protein sorting; VTI, Vps10 (ten) interacting; WT, wild-type.

to the Golgi. Moreover, we demonstrated that Btn2 is a soluble protein that localizes to LEs and mediates the retrieval of specific cargo proteins (e.g., Yif1) from LEs to the Golgi (Kama *et al.*, 2007). Btn2 binds directly to components involved in LE-Golgi protein retrieval, such as subunits of the retromer complex (e.g.,Vps26; Seaman, 2005) and the Snc1/Snc2 exo- and endocytic v-SNAREs (Protopopov *et al.*, 1993; Gurunathan *et al.*, 2000). Together, Btn2 forms a retrieval complex composed of the yeast endocytic SNARE complex (i.e., Snc1/2, Vti1, Tlg1, and Tlg2), retromer, Snx4 (a sorting nexin; Hettema *et al.*, 2003), and Yif1, a protein that is retrieved to the Golgi (Matern *et al.*, 2000; Kama *et al.*, 2007). However, Btn2 binds to only a subset of LE-Golgi–retrieved proteins, as the carboxypeptidase Y (CPY) receptor, Vps10, cannot be coprecipitated with Btn2 and is not mislocalized in *btn2*Δ cells (Kama *et al.*, 2007). This contrasts with the results obtained using yeast defective in the retromer complex, Snx4, or Ypt6 (a Rab GTPase involved in LE-Golgi transport), all of which strongly affect Vps10 and CPY sorting. Thus multiple routes are likely to be involved in LE-Golgi protein retrieval, and Btn2 may act upon a specific route (Kama *et al.*, 2007; Seaman, 2008). Interestingly, more recent work from Kryndushkin *et al.* (2008) indicated a potential role for Btn2 in the curing of specific yeast prions. Btn2 was shown to destabilize [URE3], a self-propagating amyloid form of Ure2 (a regulator of yeast nitrogen catabolism). Overexpression of *BTN2* led to the curing of only [URE3] prion aggregates, but not of [PSI+] aggregates (i.e., Sup35 prion foci; Kryndushkin *et al.*, 2008). Whether these additional functions of Btn2 overlap with its LE-Golgi sorting function remains unknown, but the Ure2-containing prion aggregates and Btn2 were shown to colocalize (Kryndushkin *et al.*, 2008), indicating that LEs might be involved in prion curing.

Here we characterize a new gene (*YHR009C*), designated *BTN3*, as encoding a Btn2-interacting protein and negative regulator of Btn2 function. By employing the yeast two-hybrid assay, immunoprecipitation (IP), and in vitro studies, we show that Btn3 interacts directly with Btn2. As the function of Btn3 was unknown, we examined its role in the regulation of Btn2 action with respect to both endosomal protein sorting and prion curing. First, we found that Btn3 interacts genetically with mutations in *VTI1*, a t-SNARE that facilitates multiple endosomal transport routes leading to and from the vacuole. Second, we found that Btn3-GFP is a cytoplasmic protein that relocalizes to LEs marked by Snx4 and Vps27 upon *BTN2* up-regulation. Third, *BTN3* overexpression mimics the deletion of *BTN2* and leads to a block in protein (i.e., Yif1 and Kex2) retrieval to the Golgi, while the deletion of *BTN3* strengthens their association with the Golgi. These results indicate that Btn3 works in an opposite manner to Btn2 and negatively regulates the retrieval of cargo from LEs to the Golgi. This effect is specific, as neither the deletion nor overexpression of *BTN3* affected the trafficking of other proteins examined. Fourth, Btn3 and the Snc1 v-SNARE compete for the same binding domain on Btn2, and in vivo data suggest that this competition controls Btn2 localization and function. Finally, Btn3 reduces the antiprion effect of Btn2, probably by sequestering Btn2 away from Ure2-containing aggregates (i.e., the proposed insoluble protein deposit compartment [IPOD]; Kaganovich *et al.*, 2008) and preventing the curing of [URE3]. Thus Btn3 is a novel negative regulator of endosome protein sorting and prion curing in yeast, and we hypothesize that its functions may be connected to Batten disease in humans.

RESULTS

Btn3 interacts with Btn2

Full-length yeast Btn2 (Kama *et al.*, 2007) was used as bait in the yeast two-hybrid screen along with a yeast cDNA library as prey. Out of ~900,000 transformants, one repetitively tested positive for *lacZ* expression and resistance to 3-aminotriazole (3AT), a metabolic inhibitor of His3 function and growth in the absence of histidine. DNA sequencing revealed that this clone carried a gene encoding a protein of unknown function (ORF *YHR009C*), which we designate as *BTN3*. Sequence alignments performed using the T-COFFEE program (Poirot *et al.*, 2003) revealed that *BTN3* from *Saccharomyces cerevisiae* is 26% identical and 51% similar to the human *FOXRED1* (FAD-dependent oxidoreductase domain containing 1) over its entire length (523 amino acids; Supplemental Figure 1). Little is known about *FOXRED1* except that it is differentially expressed during *HER-2/neu* overexpression in human breast cancer cells (Oh *et al.*, 1999), although recent work suggests that autosomal recessive mutations in *FOXRED1* lead to human complex I deficiency (Calvo *et al.*, 2010; Fassone *et al.*, 2010), a severe mitochondrial respiratory disease.

As the cellular functions of neither Btn3 nor FOXRED1 are known, we characterized the Btn2–Btn3 interaction further. Previously, this approach was successful in identifying novel SNARE-interacting proteins and their functions. For example, Btn2 was identified as a Snc1-interacting partner involved in endosomal protein sorting (Kama *et al.*, 2007). Likewise, Ddi1/Vsm1 was identified as a Snc2-interacting partner (Lustgarten and Gerst, 1999) as well as a novel ubiquitin receptor and t-SNARE binding protein (Marash and Gerst, 2003; Gabriely *et al.*, 2007), and the Gcs1 Arf-GAP was identified as a Snc2-interacting factor involved in Snc v-SNARE recycling to the Golgi (Robinson *et al.*, 2006).

We first verified the Btn2–Btn3 interaction using the two-hybrid assay. When coexpressed in yeast, the Btn3-Gal4 transactivating domain (AD) and Btn2-Gal4 DNA-binding domain (BD) fusions yielded cells able to grow in the presence of 3AT (Figure 1A), confirming that Btn3 and Btn2 interact. Subsequent bioinformatic analysis of the Btn3 sequence revealed the presence of an FAD-dependent D–amino acid oxidase domain at the C terminus (residues ~350–523) that is highly conserved in fungi and represents the most conserved region between Btn3 and FOXRED1 (Supplemental Figure 1). To better understand the role of the different regions of Btn3 in its interaction with Btn2, we constructed Btn3 truncation mutants fused to Gal4 AD (see Supplemental Figure 2A) and tested for their ability to interact with full-length Btn2 fused to the Gal4 BD. We found that the conserved C terminus of Btn3 is indispensable for binding to Btn2, as C-terminal truncation mutants (i.e., $Btn3^{1–262}$ and $Btn3^{1–393}$) did not interact with Btn2, whereas an N-terminal truncation mutant (e.g., $Btn3^{131–523}$) did interact (Figure 1A). Although we did not determine the minimum region of Btn3 responsible for Btn2 binding, the results suggest that a section downstream of residue 131 and containing residues 394–523 is likely to bear the interacting domain. Although not as stable as the AD fusion containing full-length Btn3, all of the truncation mutants could be detected by Western analysis (Supplemental Figure 2B).

We further verified the Btn2–Btn3 interaction by coIP. HA-tagged Btn3 was overexpressed from a multicopy plasmid along with myc-tagged Btn2 from a single-copy plasmid in either wild-type (WT) or *btn3*Δ yeast, and the lysates were subjected to IP with anti-myc antibodies. Western blotting of precipitates after SDS–PAGE revealed that myc-Btn2 could coprecipitate HA-Btn3 in either cell type (Figure 1B).

BTN3 interacts genetically with *VTI1*

A high-throughput interaction study by Ito *et al.* (2001) showed that YHR009c physically interacts with Vts1, a protein of unclear function that possesses DNA- and RNA-binding activities (Johnson and

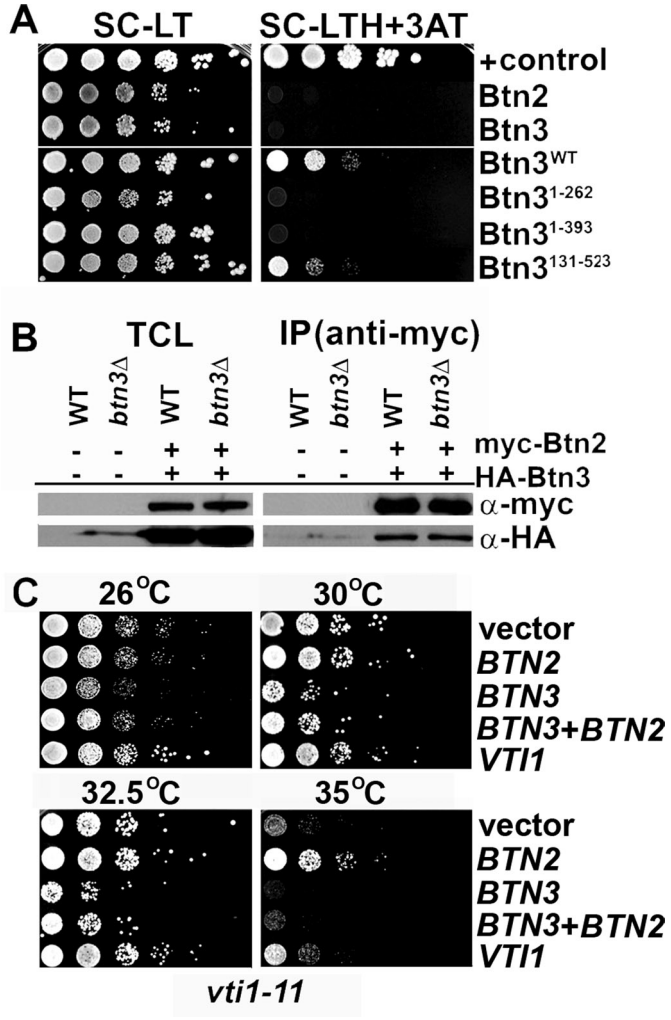

FIGURE 1: Btn3 interacts with Btn2. (A) Btn3 interacts with Btn2, as assayed by two-hybrid. Yeast (AH109) were transformed with plasmids expressing the Gal4 BD fused to full-length Btn2, the Gal4 AD fused to full-length Btn3, or both the Gal4 BD fused to full-length Btn2 (+ *Btn2*) and various Btn3 truncation mutants (as indicated) fused to the Gal4 AD. Cells were grown to mid–log phase prior to serial dilution and plating onto control medium (SC-LT) or medium lacking histidine and containing 3AT (SC-LTH + 3AT). Positive control (+ *control*) cells expressing p53 and SV40 were used in parallel. See *Materials and Methods* for more detail. (B) Btn3 coimmunoprecipitates with Btn2. WT (BY4741) and *btn3*Δ yeast expressing myc-Btn2 from a single-copy plasmid (pRS313-myc-BTN2-mRFP) and HA-tagged Btn3 from a multicopy plasmid (pAD54-BTN3), or bearing control vectors (pAD54, pRS313) alone, were grown and processed for immunoprecipitation with anti-myc antibodies. Immunoprecipitates (IP) from each reaction mixture (500 µg protein per reaction) and TCL (30 µg protein per lane) were resolved by SDS–PAGE and detected in blots with anti-myc (1:5000) and anti-HA antibodies (1:5000). (C) Overexpression of *BTN3* inhibits the growth of *vti1–11* cells. *vti1–11* cells transformed with a control vector (pAD54; *vector*) or vectors expressing *HA-BTN2* (*BTN2*), *HA-BTN3* (*BTN3*), and *HA-VTI1* (*VTI1*) from multicopy plasmids (pAD54-BTN2, pAD54-BTN3, or pAD54-VTI1, respectively), or both *HA-BTN2* and *myc-BTN3* (*BTN2+BTN3*) (pAD54-BTN2 and pRS426-myc-BTN3, respectively) were grown at 26°C before serial dilution (×10) and plating onto prewarmed medium. Plates were grown for 2–3 d at the indicated temperatures.

Donaldson, 2006; Oberstrass *et al.*, 2006; Lee *et al.*, 2010), and interacts genetically with the Vti1 Q/t-SNARE (Dilcher *et al.*, 2001). Vti1 is involved in multiple endosomal transport routes leading to and from the vacuole (i.e., Golgi to LE/prevacuolar compartment [PVC]/multivesicular body [MVB], LE/PVC to vacuole, cytosol to vacuole, retrograde LE/PVC to Golgi, and retrograde early endosome [EE] to Golgi transport) (Fischer von Mollard *et al.*, 1997; Fischer von Mollard and Stevens, 1999; Stein *et al.*, 2009), and *BTN2* overexpression enhanced the growth of temperature-sensitive *vti1–11* cells (Kama *et al.*, 2007; mistakenly written therein as *vti1–1* cells). To determine whether Btn3 has a role in protein trafficking, we first examined whether *BTN3* interacts genetically with mutations in *VTI1*. In contrast to the effect of *BTN2* overexpression, *BTN3* overexpression significantly reduced the growth of temperature-sensitive *vti1–11* mutants (Figure 1C). This reduction of growth was observed at all temperatures but was more robust at 30°C and higher. The coexpression of *BTN2* along with *BTN3* led to only a mild improvement in cell growth, indicating that elevated levels of Btn2 may not be sufficient to overcome the effect of Btn3 overproduction. We note that the overexpression of *BTN3* also inhibited the growth of *vti1–2* cells but was less pronounced (our unpublished observations). As the *vti1–11* and *vti1–2* mutants are blocked in protein transport to the LE (among other steps) at the restrictive temperature (Fischer von Mollard *et al.*, 1997; Fischer von Mollard and Stevens, 1999), the inhibition seen upon *BTN3* overexpression suggests a possible inhibitory role for Btn3 in Golgi–LE transport.

Btn3 regulates Yif1 and Kex2 localization

As Btn3 binds to Btn2 and interacts genetically with mutations in *VTI1*, we examined whether the deletion or overexpression of *BTN3* regulates protein trafficking. We examined the localization of Yif1, a Golgi protein involved in the recruitment of Ypt1 and the fusion of COPII transport vesicles with the Golgi (Matern *et al.*, 2000). This protein is mislocalized to the vacuole in *btn2*Δ cells (Chattopadhyay *et al.*, 2003; Kama *et al.*, 2007) and other strains defective in LE–Golgi transport (Kama *et al.*, 2007). Importantly, Btn2 acts along with retromer and Snx4 to mediate the retrieval of Yif1 from LEs back to the Golgi (Kama *et al.*, 2007). Here we found that GFP-tagged Yif1 expressed from a single-copy plasmid gave mainly punctate Golgi-like labeling in WT cells (Matern *et al.*, 2000; Chattopadhyay *et al.*, 2003) and accumulated in the vacuole in *btn2*Δ cells (Figure 2A), as previously shown (Kama *et al.*, 2007). However, GFP-Yif1 appeared to be better retained in punctate structures in *btn3*Δ cells, in comparison to WT cells. We determined whether these punctate structures are indeed Golgi by examining the localization of GFP-Yif1 along with DsRed-tagged Sec7, a *trans*-Golgi marker (Franzusoff *et al.*, 1991) in both WT and *btn3*Δ cells. Although DsRed-Sec7 labeled less puncta overall, probably due to its expression from the chromosome and/or slower DsRed maturation, we found that GFP-Yif1 colocalized with the DsRed-Sec7 in both cell types (Supplemental Figure 3A). This indicates that Yif1 likely remains at the Golgi in the absence of *BTN3*.

In contrast to *btn3*Δ and WT cells, *BTN3* overexpression led to the appearance of GFP-Yif1 in vacuole (Figure 2A); thus Btn3 induces Yif1 mislocalization. As the loss of Yif1 function in conditional–lethal mutants results in a block in endoplasmic reticulum (ER)-to-Golgi transport and leads to the accumulation of immature forms of cargo proteins, such as CPY, alkaline phosphatase (ALP), or invertase (Matern *et al.*, 2000), we examined whether the mislocalization of Yif1 in either *btn2*Δ cells or *BTN3* overexpressing cells leads to defects in protein processing and/secretion. We examined CPY processing by Western analysis to check the form(s) present at steady-state in lysates derived from WT, *btn2*Δ, *btn3*Δ, *BTN3* overexpressing, and control *yif1–1* and *yif1–2* cells grown at 30°C (Supplemental Figure 3B). However, neither the deletion of *BTN2* or *BTN3* nor overexpression of *BTN3* led to the accumulation of

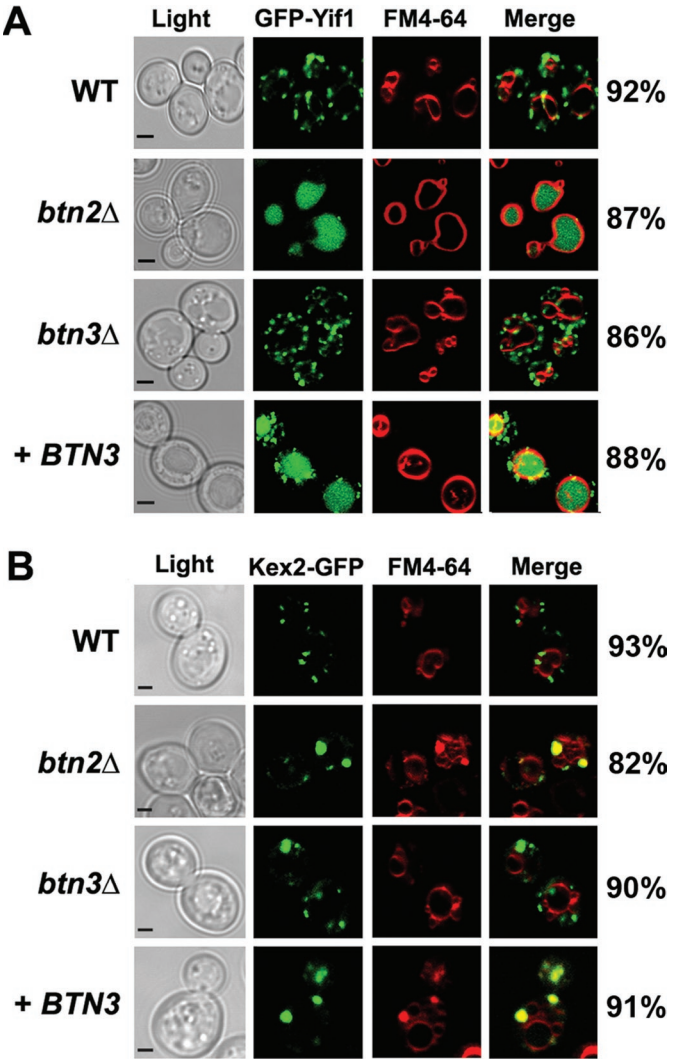

FIGURE 2: Btn3 regulates Yif1 and Kex2 localization. (A) GFP-Yif1 is mislocalized to vacuoles in cells overexpressing *BTN3*. A single-copy plasmid expressing GFP-Yif1 (pRS316-GFP-YIF1) was transformed into WT (BY4741), *btn2*Δ, *btn3*Δ, and WT cells overexpressing *BTN3* from a multicopy plasmid (pAD54-BTN3). Cells were grown at 26°C prior to pulse-chase labeling with FM4–64 (1.6 μM final concentration; 1 h at 26°C) and visualization. *Merge* indicates merger of the GFP and FM4–64 windows. Note prominent labeling of the vacuole in *btn2*Δ cells and cells overexpressing *BTN3*. Scale bar = 1 μm. Representative cells are shown, although the percentage of cells that show that specific pattern of localization is given to the right of the row (in percent), and is based on counting 100 cells for each sample; n = 3 experiments. (B) Kex2-GFP is mislocalized to late endosomes in *btn2*Δ cells and WT cells overexpressing *BTN3*. A single-copy plasmid expressing Kex2-GFP (pUG23-ADHp-KEX2-GFP) was transformed into WT, *btn2*Δ, *btn3*Δ, or WT cells overexpressing *BTN3* from a multicopy plasmid (pAD54-BTN3). Cells were grown, labeled with FM4–64, and visualized. *Merge* indicates merger of GFP and FM4–64 fluorescence windows. Statistics regarding the localization were determined as described in (A).

immature CPY (i.e., P2 form) as was seen in samples derived from temperature-sensitive *yif1–1* or *yif1–2* cells. In addition, we grew WT, *btn2*Δ, *btn3*Δ, *BTN3* overexpressing, and control *vps27*Δ cells on nitrocellulose filters and examined them for the presence of secreted CPY by immunoblotting. In contrast to *vps27*Δ cells, CPY was not secreted by *btn2*Δ, *btn3*Δ, or *BTN3* overexpressing cells at levels that differed from that of WT cells (Supplemental Figure 3C). Thus, despite Yif1 mislocalization in *btn2*Δ and *BTN3* overexpressing cells, no significant defects in protein trafficking were observed.

The localization of Kex2, a yeast subtilisin-like serine protease trafficked between the *trans*-Golgi and LE (Wilcox and Fuller, 1991; Bryant and Stevens, 1997), was also affected by the levels of either Btn2 or Btn3. GFP-tagged Kex2 (Kex2-GFP) expressed from a single-copy plasmid gave punctate Golgi-like labeling in WT cells and *btn3*Δ cells (Figure 2B). However, it was found to accumulate in LE compartments (i.e., observed adjacent to the vacuole using the lipophilic dye FM4–64) in both *btn2*Δ cells and cells overexpressing *BTN3* (Figure 2B). Kex2 functions as a protease in the *trans*-Golgi-EE that processes proteins that traverse the secretory pathway, including the α-mating factor pheromone (Julius *et al.*, 1983; Fuller *et al.*, 1989). We checked whether Kex2 mislocalization to the LE in either *btn2*Δ or *BTN3* overexpressing cells leads to defects in α-factor maturation. We performed a halo test by spotting 2.5 μl of a saturated culture of MATα WT, *btn2*Δ, *btn3*Δ, and *BTN3* overexpressing cells on a lawn of *MAT***a** *sst2*Δ tester cells (Supplemental Figure 3D). Although the deletion of *BTN3* did not affect halo size (i.e., the region where *MAT***a** cell growth is arrested), *btn2*Δ cells gave only a very small halo in comparison to WT cells. Importantly, no halo was observed around WT cells overexpressing *BTN3*. Therefore Kex2 mislocalization to the LE in both *btn2*Δ and *BTN3* overexpressing cells appears to have significant effects upon the secretion of active α-factor.

Since we previously demonstrated that Yif1 localization was unaltered in the yeast defective in endocytosis, EE-Golgi transport, LE-vacuole transport, and Golgi export (Kama *et al.*, 2007), the results shown here with both Yif1 and Kex2 indicate that Btn3 production attenuates protein retrieval from the LE to the Golgi.

Btn3 does not affect the localization of other trafficked proteins

As Btn3 appears necessary for Yif1 and Kex2 recycling, we examined whether the trafficking of other proteins is affected by the deletion or overexpression of *BTN3*. We first examined the localization of GFP-tagged PM proteins that are trafficked to endosomes and/or the vacuole. We examined the localization of Fur4, a uracil permease that recycles through LEs to the PM (Bugnicourt *et al.*, 2004). Fur4-GFP expressed from a single-copy plasmid labeled the PM and vacuole (where it is degraded) in WT cells, *btn3*Δ cells, and cells overexpressing *BTN3* (Supplemental Figure 4A). Moreover, Western blot analysis of lysates derived from these cells (using anti-GFP antibodies) indicated that there was no change in the ratio of PM localized to vacuolar Fur4-GFP at steady state (our unpublished observations). Thus Fur4 trafficking is unaltered by Btn3.

Next we examined GFP-tagged Snc1, which undergoes normal recycling from EEs to the Golgi. GFP-Snc1 expressed from a single-copy plasmid labeled the bud PM, as well as small punctate structures that correspond to EEs and the *trans*-Golgi (Lewis *et al.*, 2000; Robinson *et al.*, 2006), in WT cells, *btn3*Δ cells, and cells overexpressing *BTN3* (Supplemental Figure 4B). Thus Btn3 does not play a role in Snc1 endosomal sorting and retrieval.

We then examined the localization of GFP-tagged Ste2, the α-factor pheromone receptor, which undergoes internalization and trafficking to the vacuole in a ligand-dependent manner (Stefan and Blumer, 1999). We determined the steady-state localization of Ste2-GFP in untreated WT cells, *btn3*Δ cells, and cells overexpressing *BTN3*, but found no change in Ste2 localization either by fluorescence microscopy (Supplemental Figure 4C) or by Western analysis (our unpublished observations).

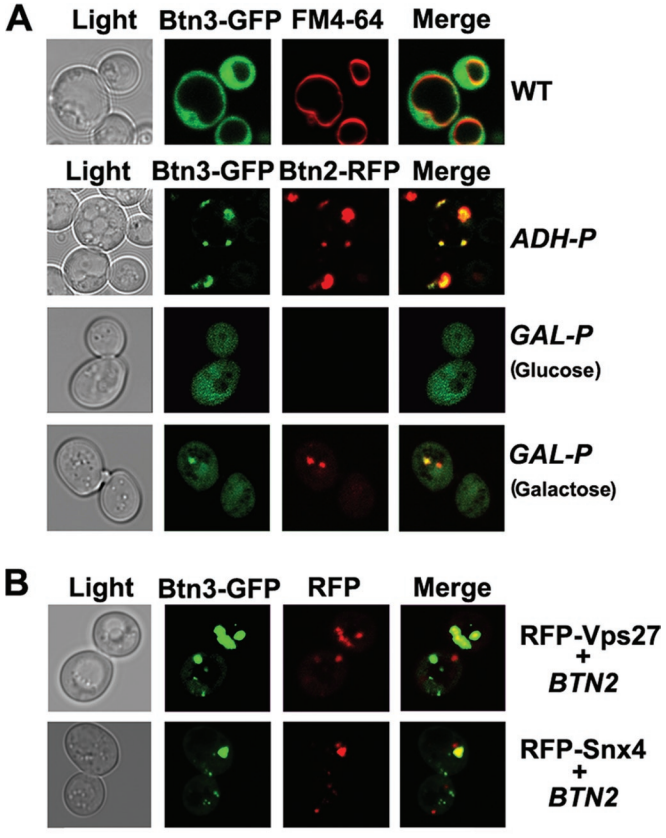

FIGURE 3: Btn2 recruits Btn3 to Vps27- and Snx4-labeled compartments. (A) Btn2 affects Btn3 localization. (Top) WT yeast (BY4741) expressing *BTN3-GFP* from a single-copy plasmid (pUG23-ADHp-BTN3-GFP) were grown at 26°C prior to pulse-chase labeling with FM4–64 and visualization. (Bottom, top row) WT yeast expressing *BTN3-GFP* from a single-copy plasmid were transformed with a single-copy plasmid expressing *BTN2-RFP* under a constitutive *ADH1* (pRS316-BTN2-mRFP) promoter and grown at 26°C prior to visualization (*ADH-P*). (Bottom, middle and bottom rows) WT yeast expressing *BTN3-GFP* from a single-copy plasmid were transformed with a multicopy plasmid expressing *BTN2-RFP* under a *GAL* promoter (pYES52-BTN2-RFP). Cells were grown to mid–log phase in SC medium containing either 2% glucose (*GAL-P* (glucose); middle row) or 2% raffinose followed by induction with galactose for 24 h (*GAL-P* (galactose); bottom row) prior to visualization. (B) Btn3 is recruited to Snx4- and Vps27-labeled compartments upon *BTN2* overexpression. WT yeast (BY4741) coexpressing *BTN3-GFP* and *BTN2* from single-copy plasmids (pUG23-ADHp-BTN3-GFP and pRS316-BTN2, respectively) were transformed with multicopy plasmids expressing either RFP-Vps27 (pAD54-mRFP-VPS27) or RFP-Snx4 (pAD54-mRFP-SNX4). Cells were grown at 26°C prior to visualization. *Merge* indicates merger between the GFP and RFP windows.

We also examined the effect of *BTN3* deletion or overexpression on the localization of proteins known to reside in the *trans*-Golgi and endosomal compartments, or those trafficked to the vacuole. We examined the localization of GFP-tagged Tlg1, Tlg2, Snx4 and Vps10 in WT cells, *btn3*Δ cells, and cells overexpressing *BTN3*. However, we observed no changes in their pattern of localization or that of Sed5, a t-SNARE that labels the *cis* Golgi (Supplemental Figure 5). In addition, neither GFP-tagged CPY nor carboxypeptidase S was mislocalized in cells lacking or overexpressing *BTN3*, nor was CPY secreted onto nitrocellulose filters, unlike control *vps* cells (Supplemental Figure 3C). Moreover, we examined whether *BTN3* overexpression altered the growth of temperature-sensitive COPI mutants (i.e., *sec21–2, sec27–1, sec28*Δ, and *sec33–1* cells), which are involved mainly in retrograde Golgi-ER trafficking; however, no additional temperature-sensitive defects were observed (Supplemental Figure 6). Finally, cells either lacking or overexpressing *BTN3* did not secrete Kar2 onto nitrocellulose filters, a phenotype observed upon defects in Golgi-ER transport (Duden *et al.*, 1994), unlike control *sec21–2* and *sec33–1* cells (our unpublished results). Thus the specific trafficking defects seen in yeast overexpressing *BTN3* (i.e., Yif1 and Kex2 mislocalization) pertain solely to defects in LE-Golgi sorting.

Btn2 recruits Btn3 to Snx4- and Vps27-labeled endosomal compartments

We examined Btn3 localization by determining where Btn3-GFP localizes in WT cells stained with FM4–64 to label the vacuolar compartments. Btn3-GFP was uniformly distributed in WT cells, with the exception of the vacuolar lumen, which was not labeled (Figure 3A, top row). However, when both Btn2-RFP and Btn3-GFP were constitutively expressed in WT yeast from single-copy plasmids, we found that they colocalized to large punctate structures (Figure 3A, second row, *ADH-P*). This was confirmed by coexpressing Btn2-RFP under a galactose-inducible promoter from a multicopy plasmid, along with Btn3-GFP from a single-copy plasmid. Before galactose induction, we observed that Btn3-GFP localized to the cytoplasm and nucleus (Figure 3A, third row, *GAL-P* (Glucose)). However, after galactose induction and *BTN2* overexpression, Btn3 relocalized to punctate structures marked by Btn2-RFP (Figure 4A, fourth row, *GAL-P* (Galactose)).

As Btn2-RFP colocalizes with LE/MVB markers, such as Snx4 and Vps27 (Kama *et al.*, 2007), we examined whether Btn3-labeled puncta are endosomes. To do this, we coexpressed Btn3-GFP and either RFP-tagged Snx4 or Vps27 in yeast overexpressing *BTN2* from a single-copy plasmid (to recruit Btn3 to the punctate structures). Under these conditions, Btn3-GFP colocalized to a large extent with both RFP-Vps27 and RFP-Snx4 (Figure 3B), indicating that Btn2 recruits Btn3 to Vps27- and Snx4-labeled endosomal compartments. Thus Btn3 is recruited to the site of Btn2 localization when the latter is overexpressed.

Btn3 overproduction sequesters Btn2 into large detergent-insoluble aggregates

As Btn3 may be a negative regulator of Btn2, we examined whether *BTN3* expression alters the localization of Btn2. To do this, we expressed Btn2-GFP from a single-copy plasmid in both WT and *btn3*Δ yeast cells and found that Btn2-GFP localized to one to two large punctate structures that also colabeled with FM4–64, as shown previously (Kama *et al.*, 2007), in both cell types (Figure 4A; note that the weak FM4–64 endosomal labeling is a likely consequence of the labeling conditions used in this study). Similar results were seen with Btn2-RFP expressed from a single-copy plasmid in WT cells (Figure 4B), as well as in *btn3*Δ cells (our unpublished observations). Thus the absence of Btn3 does not affect Btn2 localization to endosomes.

In contrast, Btn2-RFP localized to large aggregate-like structures that varied in both shape and size upon *BTN3-GFP* coexpression with *BTN2-RFP* (Figure 4C, first row), as noted earlier (Figure 3A, second row). We then examined whether the physical interaction between Btn3 and Btn2 is needed for this change in Btn3 localization, by coproducing Btn2-RFP along with various GFP-tagged Btn3 truncation mutants either bearing or lacking the Btn2-interaction domain (i.e., residues 394–523) in both WT and *btn3*Δ yeast cells. Similar results were observed with both the cell types, although only

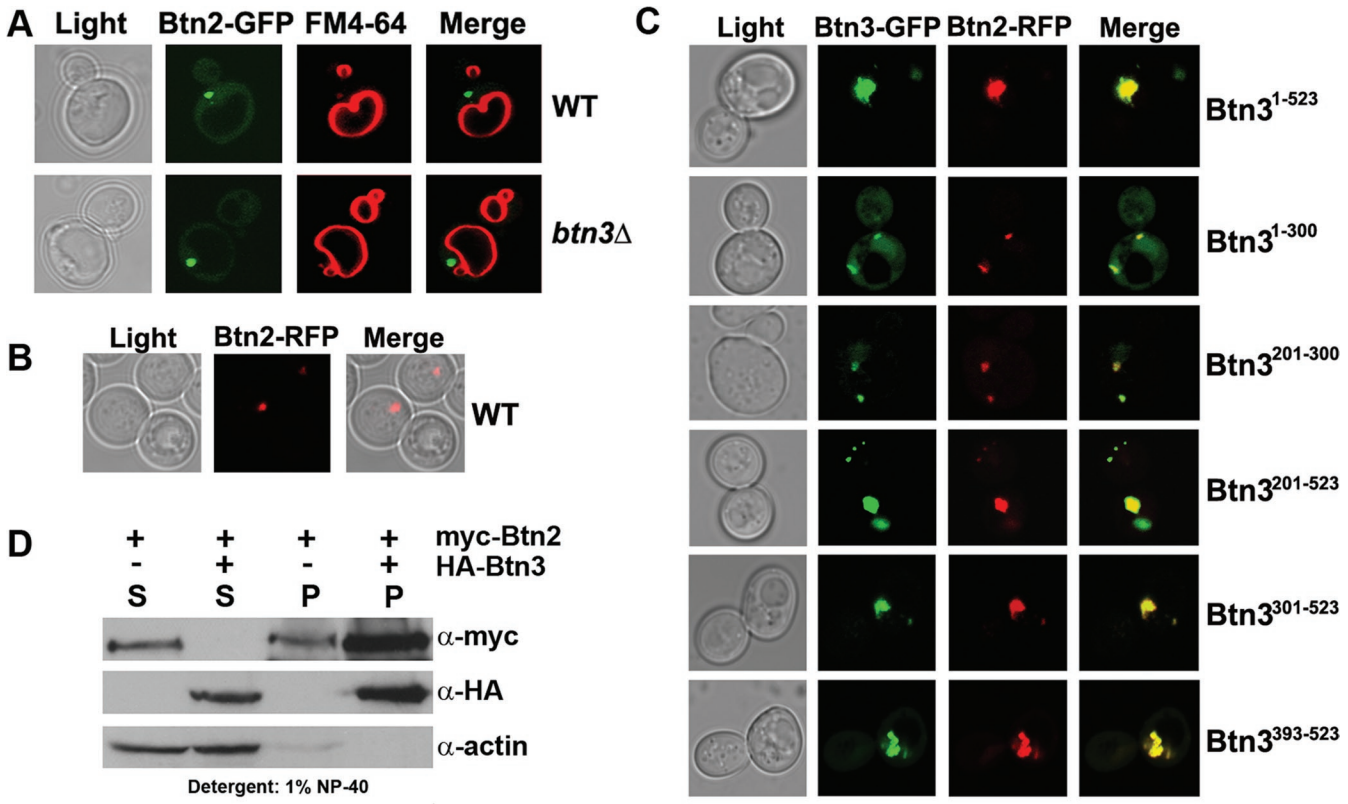

FIGURE 4: Btn3 overproduction recruits Btn2 to large detergent-insoluble aggregates. (A) The localization of Btn2 is not altered in *btn3*Δ cells. WT and *btn3*Δ cells expressing *BTN2-GFP* from a single-copy plasmid (pRS313-BTN2-GFP) were grown at 26°C prior to pulse-chase labeling with FM4–64 and visualization. *Merge* indicates the merger between the GFP and FM4–64 fluorescence windows. (B, C) *BTN3* overexpression alters the localization of Btn2. WT yeast were transformed with a plasmid expressing full-length *BTN2* fused to *RFP* from a single-copy plasmid (*Btn2-RFP*; pRS313-BTN2-mRFP) either alone (B) or together with either full-length Btn3 (residues 1–523; pUG35-ADHp-Btn3$^{1–523}$-GFP) or a Btn3 truncation mutant fused to GFP (C), as indicated. Cells were grown at 26°C prior to visualization. *Merge* indicates merger between the GFP and RFP fluorescence windows. (D) Btn2 is recruited to the detergent-insoluble pellets in the presence of overproduced Btn3. WT yeast were transformed with a single-copy plasmid producing myc-tagged Btn2 fused to RFP (*myc-Btn2*; pRS313-myc-BTN2-mRFP) either alone or together with a multicopy plasmid producing full-length HA-tagged Btn3 (*HA-Btn3*; pAD54-BTN3). Cells were grown to mid–log phase and processed by cell fractionation to yield pellet (*P*) and supernatant fractions (*S*) (see *Materials and Methods*) that were resolved by SDS–PAGE and detected in blots using anti-HA and anti-myc antibodies. Actin was detected in parallel as a loading control using anti-actin antibodies.

the results from the WT cells are shown (Figure 4C). Therein, we observed the aggregation of Btn2-RFP in the presence of those Btn3 mutants that contain the putative Btn2-interacting region (i.e., Btn3$^{201–523}$, Btn3$^{301–523}$, and Btn3$^{393–523}$) (Figure 4C). In contrast, typical LE-like labeling with Btn2 was observed in the control cells (Figure 4B) and cells expressing those Btn3-GFP mutants that lack the putative Btn2-interaction region (i.e., Btn3$^{1–300}$ and Btn3$^{201–300}$; Figure 4C). This indicates that a physical interaction between Btn3 and Btn2 is necessary for altering the cellular localization of Btn2. However, a direct interaction is not required for the recruitment of Btn3 to endosomal structures, as both Btn3$^{1–300}$ and Btn3$^{201–300}$ colocalize with Btn2, although we note that no large aggregates were observed in these cells (Figure 4C, second and third rows). Therefore we determined whether Btn2 and Btn3 are detergent-insoluble in cells that contain the aggregates. We used Western analysis to check for the presence of Btn2 in the detergent-soluble or -insoluble fractions (i.e., pellet) from cells expressing only myc-tagged Btn2 from a single-copy plasmid or together with HA-tagged Btn3 from a multicopy plasmid. The results indicate that myc-Btn2, which is distributed equally to the detergent-soluble and -insoluble fractions in the absence of exogenous *BTN3*, is highly enriched in the detergent-insoluble fraction in the presence of overproduced Btn3 (Figure 4D). Moreover, Btn3 was also found to be enriched in the detergent-insoluble fraction in these cells. Together the results indicate that Btn3 overproduction sequesters Btn2 into large detergent-insoluble aggregates.

Btn3 and Snc1 compete for the same domain on Btn2

As Snc1 also interacts physically with Btn2 (Kama *et al.*, 2007), we examined whether it plays a role in the Btn3-Btn2 association. To determine the binding sites for Btn3 and Snc1 on Btn2, we created various Btn2 truncation mutants fused to the Gal4 DB domain (schematically represented in Supplemental Figure 7A; expression levels are shown in Supplemental Figure 7B) and tested for their ability to interact with full-length Btn3 or Snc1$^{3–94}$ fused to the Gal4 AD in the yeast two-hybrid assay. As shown previously, both full-length Btn3 and Snc1 interacted with full-length Btn2 (e.g., Btn2$^{1–410}$), as assessed by growth on medium containing 3AT (Figure 5A). We also found that both Snc1 and Btn3 bind to the same domain on Btn2 that spans from residues 100–239, whereas the amino-terminal (i.e., residues 1–100) and carboxyl-terminal regions of Btn2 (i.e., residues 240–410) were both dispensable for binding (Figure 5A).

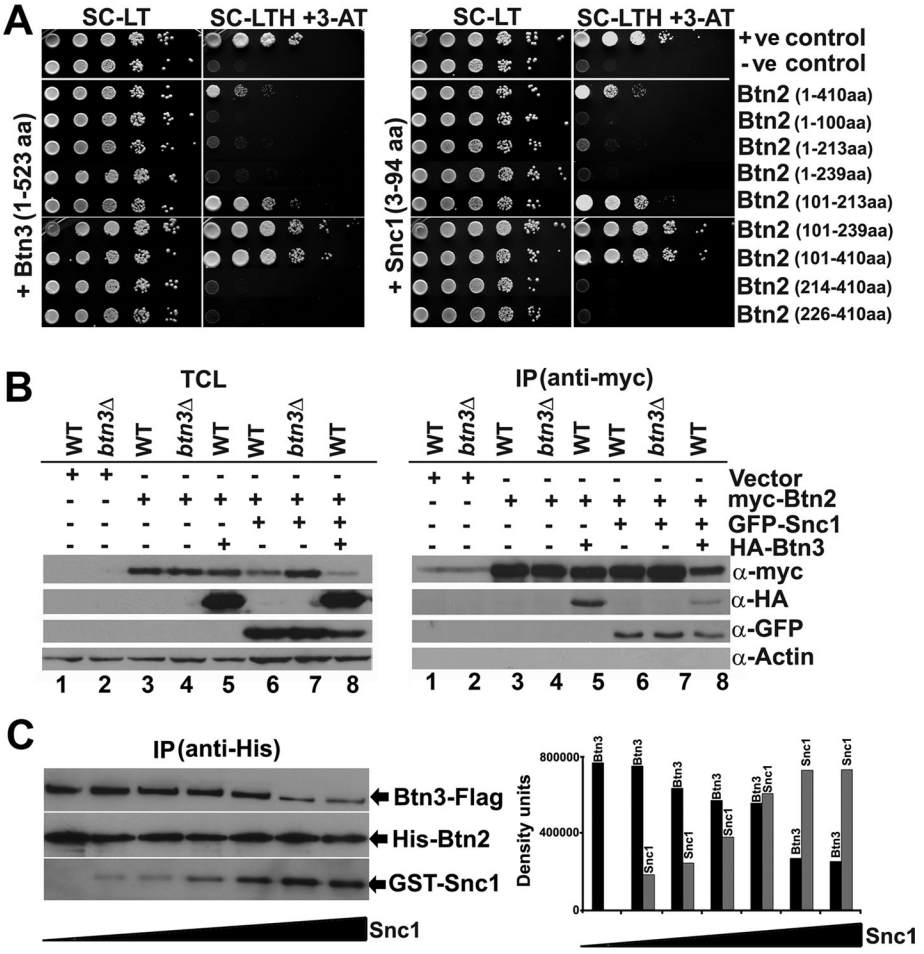

FIGURE 5: Btn3 and Snc1 compete for the same binding region on Btn2. (A) Btn3 and Snc1 bind to same domain on Btn2, as determined by two-hybrid. Yeast (AH109) were transformed with plasmids producing either full-length Btn3 (1–523 aa) or Snc1 lacking its transmembrane domain (3–94 aa) fused to the Gal4 AD, and either full-length Btn2 (1–410 aa) or one of the Btn2 truncation mutants fused to the Gal4 DB, as indicated. Cells were grown to mid–log phase prior to serial dilution (×10) and plating onto control medium (SC-LT) or medium lacking histidine and containing 16 mM 3AT (SC-LTH + 3AT). Positive control (+ control) cells expressing p53 and SV40, and negative control cells (− control) expressing full-length Btn3 (left) or $Snc1^{3–94}$ (right) together with a control empty vector were used in parallel. (B) *SNC1* overexpression inhibits the Btn3-Btn2 interaction. WT (BY4741; WT) and *btn3*Δ cells expressing *myc-BTN2* from a single-copy plasmid (pRS313-myc-BTN2-mRFP) were transformed with a multicopy plasmid expressing *HA-BTN3* (pAD54-BTN3) and a single-copy plasmid expressing *GFP-SNC1* (pUG36-ADHp-GFP-SNC1), or with each one separately. WT and *btn3*Δ cells transformed with the single-copy plasmid expressing *myc-BTN2* or with empty vectors were used as controls. Cells were grown and processed for immunoprecipitation with anti-myc antibodies. Precipitates (IP) formed from each reaction (500 µg protein per reaction) and TCLs (30 µg protein per lane) were resolved by SDS–PAGE and detected in blots with anti-myc (1:5000), anti-HA (1:5000), anti-GFP (1:1000), and anti-actin (1:10,000) antibodies (α). Note that upon GFP-Snc1 overexpression, myc-Btn2-RFP precipitated lower amounts of HA-Btn3. (C) Snc1 displaces Btn3 binding to Btn2. His_6-Btn2 and MBP-Btn3-Flag (3.6×10^{-11} and 3.0×10^{-11} moles, respectively) were mixed with increasing amounts of GST-$Snc1^{3–94}$ (between 0.2 and 12.8×10^{-11} moles) and incubated overnight at 4°C (see *Materials and Methods*). Nickel-charged beads were used to precipitate complexes that were resolved by SDS–PAGE and detected using anti-GST (1:500), anti-His_6 (1:1000), or anti-Flag (1:1000) antibodies.

Interestingly, addition of the first 100 amino terminal residues to the 101–239 interacting domain (e.g., $Btn2^{1–239}$) severely reduced its ability to interact with either Snc1 or Btn3 and may constitute an inhibitory domain.

As the above results indicate that Snc1 and Btn3 use the same binding domain on Btn2, we hypothesized that Snc1 and Btn3 compete for binding to Btn2. To verify this, we expressed a myc-tagged form of Btn2 from a single-copy plasmid in WT cells, *btn3*Δ cells, and cells overexpressing a HA-tagged form of Btn3 from a multicopy plasmid, and we performed IP with anti-myc antibodies. Western blotting of the total cell lysates and precipitates after SDS–PAGE revealed that the expression levels of myc-Btn2 were unaltered by either the deletion or overexpression of Btn3 (for a representative experiment, see Figure 5B, left panel, lanes 3–5) and that myc-Btn2 could pull down HA-Btn3 (Figure 5B, right panel, lane 5). However, when the IP experiment was performed using cells that also overexpressed *GFP-SNC1* (from a single-copy plasmid), we noted changes in the expression levels of myc-Btn2 in both *btn3*Δ cells and cells overexpressing *BTN3*, in comparison to WT cells. It was consistently observed (in repetitive experiments) that, in the presence of excess GFP-Snc1, higher levels of myc-Btn2 were observed in cells lacking *BTN3*, whereas lower levels were observed in cells overexpressing *BTN3* (Figure 5B, left panel, lanes 6–8). Correspondingly, the elevated GFP-Snc1 levels correlated with a decrease in the amount of HA-Btn3 that could be precipitated by myc-Btn2 (Figure 5B, right panel, lane 8). Because *myc-BTN2* was expressed using a constitutive promoter in all cells, this indicates that Snc1 overproduction somehow regulates the steady-state levels of Btn2 relative to the amount of Btn3 present in the cell, but probably not through changes in gene expression. Importantly, because less Btn3 was bound to Btn2 in the presence of (overproduced) GFP-Snc1, it indicates that these proteins may compete for the same binding site in vivo.

To confirm this, we performed an in vitro competition-binding assay. We produced purified recombinant His_6-tagged Btn2, GST-Snc1, and maltose-binding protein-Btn3-Flag (MBP-Btn3-Flag) from *Escherichia coli*. Recombinant Snc1 contained its soluble amino-terminal portion and SNARE-binding motif but lacked its transmembrane domain, whereas full-length Btn3 was fused with MBP at the amino-terminal to facilitate purification and a Flag tag at its carboxyl-terminal for detection. As Factor-Xa treatment of MBP-Btn3-Flag led to its fragmentation (our unpublished observations), we used the intact fusion protein in the binding assay. We first tested whether GST or MBP alone bind to Btn2 by mixing equal amounts of His_6-Btn2 and either purified recombinant GST or MBP, but did not see any physical interaction (Supplemental Figure 7C) in pull-downs with nickel beads. In contrast, we found that His_6-Btn2 bound to both GST-Snc1, as shown previously (Kama *et al.*, 2007), and MBP-Btn3-Flag. We determined the stoichiometry

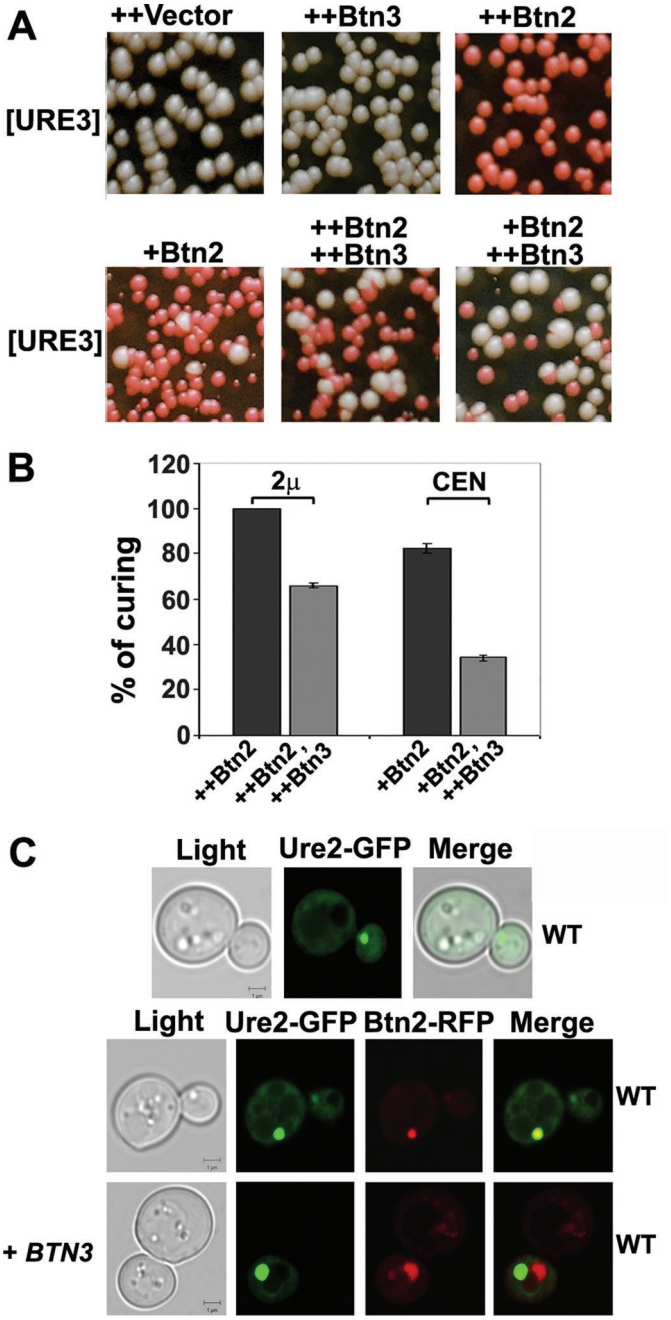

FIGURE 6: *BTN3* overexpression inhibits Btn2-mediated prion curing. Btn3 inhibits prion curing. (A) [URE3] cells (BY241) expressing *BTN2* from a multicopy plasmid (++Btn2; pAD54-BTN2) or from a single-copy plasmid (+Btn2; pRS316-BTN2-RFP) were transformed with a multicopy plasmid expressing Btn3 (++Btn3; pRS426-myc-BTN3 or pAD54-BTN3, respectively). In addition, BY241 cells were transformed with control plasmids (++vector; pAD54 and pRS426). Cells were grown overnight in YPD at 26°C, prior to dilution and plating on 0.5× YPD plates (to yield 500–750 colonies per plate). Plates were incubated at 26°C for 5 d and prion curing was determined: red colonies indicate prion loss, and white colonies are [URE3]. (B) Dose-dependent reduction of the anti-prion activity of Btn2 by Btn3. Data from (A) are represented graphically; the percentage of curing in cells that expressed Btn2 alone or together with Btn3 is shown using black- and gray-colored boxes, respectively. As in (A), 2μ (or ++) indicates *BTN2* expression from a multicopy plasmid, and CEN (or +) indicates expression from a single-copy plasmid. (C) *BTN3* overexpression reduces the colocalization of Ure2-GFP and Btn2-RFP. WT yeast expressing *URE2-GFP* under a *GAL* promoter from a multicopy plasmid (pESC-URE2-GFP) alone (top row) or with *BTN2-RFP* from a single-copy plasmid (pRS313-BTN2-RFP) (middle row) or with both *BTN2-RFP* and *BTN3* from a multicopy plasmid (pAD54-BTN3) were grown overnight in medium containing 2% raffinose and 2% glucose as a carbon source, prior to induction with 3.5% galactose. Localization of the Ure2-GFP and Btn2-RFP was visualized after 24 h of galactose induction. *Merge* indicates the merger either between the light microscopy and GFP fluorescence windows (top row) or the GFP and RFP fluorescence windows (middle and bottom rows).

of the Snc1-Btn2 and Btn3-Btn2 interactions by incubating a fixed amount of recombinant His_6-Btn2 (e.g., 3.2×10^{-11} moles) with increasing amounts of either GST-Snc1 or MBP-Btn3-Flag (i.e., $0.2–12.8 \times 10^{-11}$ moles; see representative experiment shown in Supplemental Figure 7, D and E). To measure the molar equivalents of the precipitated GST-Snc1, MBP-Btn3-Flag, and bound His_6-Btn2 in the binding assay, we used purified GST-Snc1, MBP-Btn3-Flag, and His_6-Btn2 as protein standards that were detected in parallel by Western blotting and plotted by linear regression (data not shown). This quantitative analysis revealed that both GST-Snc1 and MBP-Btn3-Flag interact with His_6-Btn2 in vitro at a ratio of 1:1 (i.e., saturation of GST-Snc1 and MBP-Btn3-Flag binding to His_6-Btn2 occurred at $\sim 3 \times 10^{-11}$ moles in both cases) (Supplemental Figure 7, D and E).

We examined whether increasing amounts of GST-Snc1 could displace MBP-Btn3-Flag binding to His_6-Btn2 in vitro (Figure 5C). We used increasing amounts of recombinant GST-tagged Snc1 (i.e., $0.2–12.8 \times 10^{-11}$ moles) in binding reactions containing equal amounts of prebound MBP-Btn3-Flag and His_6-Btn2 (e.g., 3.2×10^{-11} moles each). As the concentration of Snc1 increased, we noted a strong corresponding decrease in the amount of recombinant Btn3 bound to Btn2 (Figure 5C). Thus Snc1 acts as a competitive inhibitor of Btn3–Btn2 interaction in vitro.

BTN3 overexpression inhibits Btn2-mediated [URE3] prion curing

Aside from the retrieval of specific cargo molecules (e.g., Yif1 and Kex2) from the LE to the Golgi (Kama *et al.*, 2007 and here), Btn2 was shown to cure cells of aggregated Ure2 (i.e., [URE3] prions; Kryndushkin *et al.*, 2008). Because Btn3 acts as a negative regulator of Btn2, we examined whether Btn3 also affects [URE3] prion curing by Btn2. We used BY241 yeast, which bears *ADE2* under the control of the *DAL5* promoter (Brachmann *et al.*, 2005), in order to monitor the activity of Ure2. In these cells, *ADE2* transcription is active in the [URE3] prion state, resulting in white colonies on adenine-limiting medium, whereas nonaggregated active Ure2 represses transcription and makes the strain appear red.

First, we expressed *BTN2* from either a single- or multicopy plasmid under the constitutive *ADH1* promoter in BY241 cells and found that the lower expression of *BTN2* led to ~85% prion curing, whereas higher expression led to near-complete curing after 5 d (Figure 6, A and B), as shown previously (Kryndushkin *et al.*, 2008). Next we determined whether Btn3 has any prion curing effect by expressing it from a multicopy plasmid in BY241 cells on adenine-limiting medium. We found that all *BTN3* overexpressing colonies remained white even after several days of growth, like control cells transformed with vector alone (Figure 6A). This indicates that Btn3 does not have anti-prion activity. We then determined whether Btn3 regulates the Btn2 anti-prion activity by coexpressing *BTN3* from a multicopy

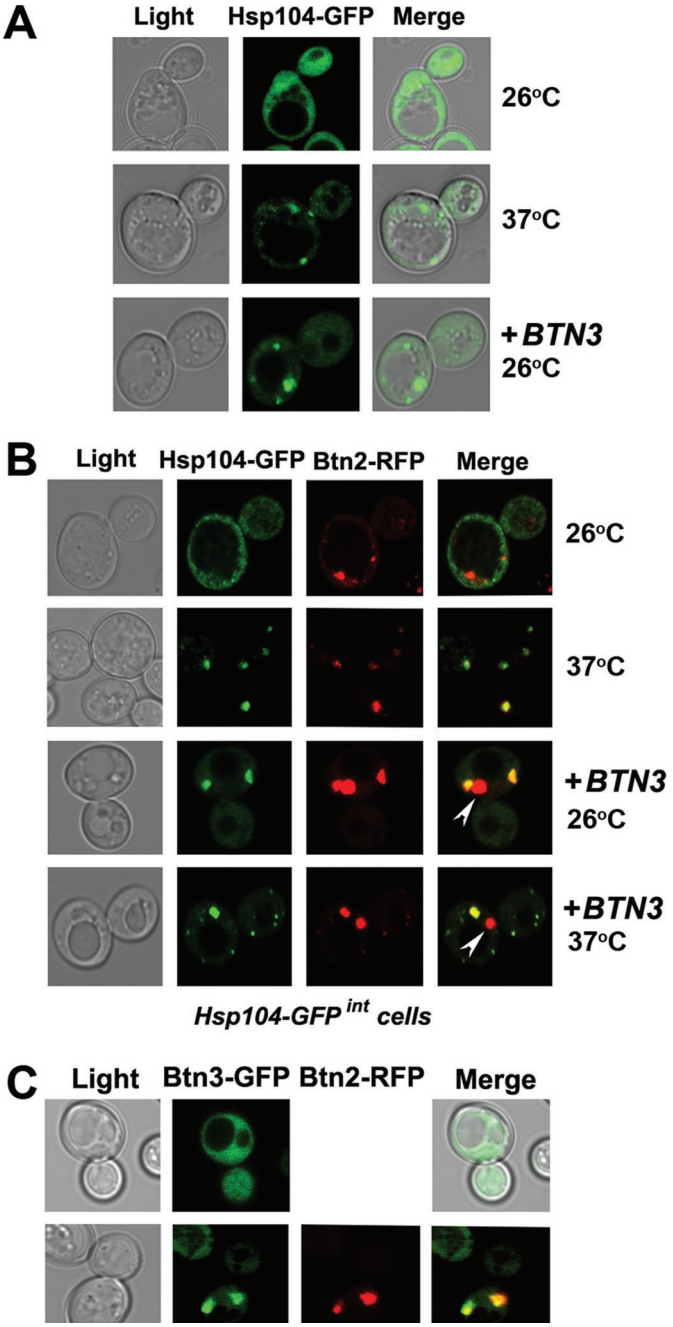

FIGURE 7: Btn3 regulates Hsp104 and Btn2 colocalization. (A) *BTN3* recruits Hsp104-GFP. Yeast expressing *HSP104-GFP* from its genomic locus were transformed either with a multicopy plasmid expressing *BTN3* (pAD54-BTN3) or vector alone (pAD54). Cells were grown at 26°C and either maintained at 26°C or shifted for 20 min to 1 h to 37°C, prior to visualization. *Merge* indicates merger between the light microscopy and GFP fluorescence windows. (B) *BTN3* overexpression relocalizes Btn2 to a non–Hsp104-labeled compartment. Yeast expressing *HSP104-GFP* from its genomic locus and *BTN2-RFP* from a single-copy plasmid (pRS316-BTN2-RFP) were transformed either with a multicopy plasmid expressing *BTN3* (pAD54-BTN3) or with a control vector (pAD54). Cells were grown as described above. *Merge* indicates merger between the GFP and RFP fluorescence windows. (C) Snc1 is a competitive inhibitor of the Btn2-Btn3 interaction in vivo. WT yeast expressing *BTN3-GFP* from a single-copy plasmid (pUG23-ADHP-Btn3-GFP; top row) were transformed with a single-copy plasmid expressing Btn2-RFP (pRS316-Btn2-RFP; middle row), and in addition with a multicopy plasmid expressing *SNC1* (pAD54-SNC1; bottom row). Cells were grown at 26°C prior to visualization. *Merge* indicates merger of the light and fluorescence microscopy images (top row) and the GFP and RFP fluorescence windows (other rows).

BTN2 (2μ)	*BTN2* (CEN)	*BTN3* (2μ)	*BTN2* (2μ) + *BTN3* (2μ)	*BTN2* (CEN) + *BTN3*(2μ)
100	84.1 ± 4.0	0	64.6 ± 3.5	34.7 ± 4.2

Full-length *BTN3* and *BTN2* were expressed under the control of an *ADH1* promoter in BY241 [URE3] either alone or together as represented in first row. 2μ indicates expression from a multicopy plasmid (i.e., pAD54-BTN2 and/or pRS426-myc-BTN3), and CEN represents expression from a single-copy plasmid (pRS316-BTN2-RFP). Cells were plated on 0.5× YPD plates, and prion loss was determined by colony counting after 5 d of incubation at 26°C. Numbers in the table indicate the average percentage of cured colonies for each combination (% ± SD; n = 3 independent experiments).

TABLE 1: Btn3 inhibits [URE3] prion curing by Btn2.

plasmid along with *BTN2* from either a single- or multicopy plasmid. We found that Btn3 overproduction decreased the percentage of prion curing by Btn2 by >1.5-fold (e.g., to ~65% curing, n = 3; Table 1) when both are expressed from multicopy plasmids, whereas it decreased curing by 2.4-fold (e.g., to ~35% curing, n = 3) when *BTN3* is expressed from a multicopy plasmid and *BTN2* from a single-copy plasmid (Figure 6, A and B; Table 1). Thus Btn3 negatively regulates dosage-dependent [URE3] prion curing by Btn2.

Btn3 controls the ability of Btn2 to localize with the IPOD

Btn2-RFP colocalization with [URE3] prion aggregates was shown to be required for efficient prion curing (Kryndushkin *et al.*, 2008). Also, Btn2 mutants showing a normal pattern of localization (i.e., one to two puncta per cell) had higher curing rates in comparison to those mutants showing multiple and larger puncta (Kryndushkin *et al.*, 2008). As Btn3 overexpression results in the aberrant localization of Btn2-RFP to multiple and larger puncta/aggregates (Figures 3A and 4C), we examined whether Btn3 overexpression alters the colocalization of Btn2-RFP and Ure2-GFP aggregates (Figure 6C). First, we overexpressed *URE2-GFP* from a multicopy plasmid under galactose-inducible promoter and found that, after 24 h of induction on galactose-containing medium, it localized to aggregate-like punctate structures (Figure 6C, upper panel), as shown previously (Kaganovich *et al.*, 2008). We then expressed *BTN2-RFP* from a single-copy plasmid in *URE2-GFP*–expressing cells and found that they colocalized to the same structure (Figure 6C, middle panel), as expected. However, when *BTN3* was overexpressed (from a multicopy plasmid) along with *BTN2-RFP* and *URE2-GFP*, the majority of Btn2-RFP localized to granular structures devoid of Ure2-GFP, whereas only a small visible amount of Btn2-RFP colocalized with the Ure2-GFP aggregates (Figure 6C, lower panel). This indicates that Btn3 could negatively regulate the anti-prion activity of Btn2 by altering its localization (i.e., away from Ure2-GFP aggregates).

As Ure2 aggregates mark the IPOD (Bagola and Sommer, 2008; Kaganovich *et al.*, 2008) and colocalize with Btn2 (Figure 6C; Kryndushkin *et al.*, 2008), it is possible that Btn2 also associates with this compartment where protein aggregates and/or amyloids are proposed to be sequestered (Kaganovich *et al.*, 2008) and has been speculated to be the site of prion induction de novo (Tyedmers *et al.*, 2010). Therefore *BTN3* overexpression could alter the localization of Btn2 from IPOD to non–IPOD compartments. To confirm this idea, we examined the colocalization of Btn2-RFP with Hsp104-GFP, a heat-shock protein involved in protein disaggregation

(Mosser *et al.*, 2004; Schaupp *et al.*, 2007), that localizes to the IPOD and juxtranuclear quality control (JUNQ) compartments at elevated temperatures (Kaganovich *et al.*, 2008). Although Hsp104-GFP localized mainly to the cytoplasm in WT cells (Figure 7A, first row) and in cells expressing *BTN2-RFP* from a single-copy plasmid (Figure 7B, first row), it was recruited to punctate structures (Figure 7A, second row) that colocalize with Btn2-RFP upon the shift to elevated temperatures (i.e., 37°C for 20 min) (Figure 7B, second row). These structures are likely to be IPOD compartments. However, we noted that, upon *BTN3* overexpression, Hsp104-GFP was recruited to punctate structures at 26°C in around 60% of cells (Figure 7A, third row). We also observed that, upon *BTN3* overexpression, Btn2-RFP also labeled punctate structures that were devoid of Hsp104-GFP (Figure 7B, third row). This was observed in ~60% of the cells and was independent of temperature. We also noted that numerous small Hsp104-labeled puncta were observed at higher temperatures (i.e., 37°C; Figure 7B, fourth row). These results suggest that Btn3 controls Btn2 localization and has the ability to remove Btn2 from Ure2- and Hsp104-containing compartments.

As Btn2 colocalizes with both LE/MVB markers, such as Snx4 and Vps27 (Kama *et al.*, 2007), and IPOD markers, such as Ure2 and Hsp104 (Figure 6C, middle row; and Figure 7B, second row), we examined whether Hsp104-GFP also colocalizes with Snx4 upon elevated temperatures. RFP-Snx4 partially colocalized with Hsp104-GFP at 37°C (Supplemental Figure 8A, second row), indicating that the LE and IPOD compartments may overlap. We confirmed this by examining the colocalization of RFP-Snx4 with the GFP-tagged von Hippel-Lindau tumor suppressor (VHL) in proteasome-inhibited *cim3–1* mutants. GFP-VHL localizes to the JUNQ compartment in *cim3–1* cells at permissive temperatures but relocalizes to both the JUNQ and IPOD compartments upon a shift to 37°C (Kaganovich *et al.*, 2008). At 26°C, we observed half of the cells as having GFP-VHL localized to either one or two compartments (first and second rows), which did not colocalize with RFP-Snx4 (Supplemental Figure 8B). This indicates that the JUNQ and endosomal compartments do not overlap under these conditions. However, GFP-VHL localized to either one (see fourth row) or two (see third row) compartments that colabeled with RFP-Snx4 (i.e., IPOD) at the elevated temperature. Moreover, GFP-VHL localized to multiple compartments, some partially colabeled with RFP-Snx4, in ~20% of cells (see fifth row). Thus we speculate that the IPOD and endosomes overlap under certain conditions.

Btn2 and Btn3 affect Ure2 aggregate size and number

As Btn3 might also control the localization of Hsp104, which disaggregates [URE3] prions into short infectious prion seeds (Shorter and Lindquist, 2006), we determined whether Btn3 affects the formation of Ure2 aggregates. To do this, we expressed *URE2-GFP* under a galactose-inducible promoter in WT cells, *btn3*Δ cells, and cells overexpressing either *BTN2* or *BTN3*, and examined Ure2 aggregate size and number. Interestingly, Ure2-GFP aggregates formed within 24 h in WT cells, whereas they took 37 h to form in *btn3*Δ cells, indicating that Btn3 may suppress aggregation (our unpublished observations). The formation of Ure2-GFP aggregates also occurred within 24 h in cells overexpressing either *BTN2* or *BTN3*, but the aggregates varied noticeably in both size and number (Supplemental Figure 9, A and B). Ure2-GFP aggregates were much smaller in size and number in cells overexpressing *BTN2* (Supplemental Figure 9A, second row) as compared with WT cells (Supplemental Figure 9A, first row) and those overexpressing *BTN3*, wherein a substantial number of cells had either numerous smaller aggregates or very large aggregates along with numerous smaller ones (Supplemental Figure 9A, third row). Thus Btn3 appears to increase Ure2-GFP aggregate formation, presumably by acting as a negative regulator of Btn2 targeting to Ure2-GFP aggregates.

The Snc1 v-SNARE interferes with Btn3-mediated regulation of Btn2

Because Snc1 is a competitive inhibitor of the Btn3–Btn2 interaction in vitro (Figure 5C), we examined whether this is true in vivo. For this, we first determined the effect of *SNC1* overexpression on the recruitment of Btn3-GFP to Btn2-RFP–labeled compartments (Figure 7C). Btn3-GFP expressed from a single-copy plasmid labeled the cytoplasm (Figure 7C, top row), whereas it colocalized with Btn2-RFP to large puncta upon *BTN2-RFP* expression from a single-copy plasmid (Figure 7C, second row), as shown above (Figure 4A). However, upon *SNC1* co-overexpression from a multicopy plasmid (Figure 7C, bottom row), Btn2-RFP and Btn3-GFP colocalized with much smaller and less numerous punctate structures. The results indicate that Snc1 may regulate the size and nature of Btn3-Btn2–containing structures and, perhaps, might alleviate the Btn3-mediated Btn2 relocalization seen in Figure 6C.

Next we determined whether Snc1 overproduction could block Btn3-mediated inhibition of prion curing by Btn2. We expressed *SNC1* from a multicopy plasmid in BY241 cells and found that the colonies remained white, like the control cells, on adenine-limiting medium. This indicates that Snc1 itself does not have anti-prion activity. We then coexpressed *SNC1* along with *BTN2* and *BTN3* (under a galactose-inducible promoter) from multicopy plasmids in BY241 [URE3] cells and performed the prion curing assay. We found that, in presence of excess Snc1, Btn3 reduced Btn2-mediated prion curing by 1.2-fold as compared with 1.6-fold in the absence of Snc1 (a decrease of ~45% in the inhibition of curing, n = 2; Table 2). These results confirm that Btn3 regulates the anti-prion activity of Btn2 and that Snc1 is a competitive inhibitor of the Btn2–Btn3 interaction in vivo.

DISCUSSION

Despite the numerous studies on Batten disease–related genes, the nature and mechanism of disease onset is still obscure. By employing a yeast model, we previously demonstrated that Btn2, whose gene is up-regulated in the absence of the yeast *CLN3* (the Batten

Time (h)	SNC1	BTN3	SNC1 + BTN3	BTN2	BTN2 + BTN3	BTN2 + BTN3 + SNC1
0	0	0	0	1 ± 1	0.5 ± 0.7	0.5 ± 0.7
30	0	0	0	60.1 ± 6.2	37.5 ± 7.7	50.2 ± 5.6

Full-length *SNC1* (pTGAL-HA-SNC1), *BTN3* (pYES51-BTN3), and *BTN2-RFP* (pYES52-BTN2-RFP) were expressed under the control of a galactose-inducible *GAL1* promoter in BY241 [URE3] cells either alone or together, as indicated. See *Materials and Methods* for details regarding expression. Cells were plated on 0.5× YPD plates, and prion loss was determined by colony counting after 5 d. The first column indicates the time of induction on galactose, and numbers in other columns indicate the average percentage of cured colonies for each combination (% ± SD; n = 2 independent experiments).

TABLE 2: *SNC1* overexpression partially alleviates Btn3-mediated inhibition of [URE3] prion curing by Btn2.

disease gene orthologue) (Pearce *et al.*, 1999) and is also involved in prion curing (Kryndushkin *et al.*, 2008), is actually a component of a LE-Golgi retrieval complex involved in the recycling of specific proteins (Kama *et al.*, 2007). This suggested that Batten disease and defects in prion curing necessitate intact endosomal protein sorting and retrieval.

In this study, we used a genetic screen for Btn2-interacting partners and identified an uncharacterized ORF, designated here as *BTN3*. *BTN3* encodes a conserved oxidoreductase of unknown function, but whose orthologue in humans, *FOXRED1*, was recently shown to be mutated in patients with human complex I deficiency (Calvo *et al.*, 2010; Fassone *et al.*, 2010). In our work, we found that Btn3 is a negative regulator of Btn2 and its functions in both endosomal protein sorting and prion curing. Few, if any, negative regulators of endosomal protein sorting have been described, although several lines of evidence imply that Btn3 is one. First, the overexpression of *BTN3* in cells bearing a temperature-sensitive *vti1–11* allele resulted in the inhibition of cell growth (Figure 1C) at elevated temperatures, in contrast to the rescue conferred by the overexpression of either *VTI1* or *BTN2* (Figure 1C). This phenotype is allele-specific, as *BTN3* overexpression only slightly inhibited the growth of cells bearing a *vti1–2* allele (our unpublished results), which is defective in protein transport to the LE and in vesicle fusion with vacuole at restrictive temperatures. *vti1–11* cells, on the other hand, exhibit defects in the retrograde trafficking of proteins to the *cis* Golgi apart from those shown by the *vti1–2* allele at restrictive temperatures (Fischer von Mollard and Stevens, 1999). Second, the overexpression of *BTN3* resulted in the accumulation of specific Golgi resident proteins (i.e., Yif1 and Kex2) in vacuoles and LE, respectively, as seen in *btn2*Δ cells (Kama *et al.*, 2007; Figure 2). In contrast, however, the deletion of *BTN3* resulted in a higher retention of GFP-Yif1 in what is probably Golgi (Figure 2A, Supplemental Figure 3A). This appears to be highly specific, as neither the overexpression nor deletion of *BTN3* affected the trafficking of a wide variety of Golgi and endosomal proteins like Sed5, Tlg1, Tlg2, Vps10, Snx4 (Supplemental Figure 5); PM proteins that cycle through endosomes, such as Snc1, Fur4, and Ste2 (Supplemental Figure 4); or vacuole-targeted proteins that use the MVB pathway, such as CPS and CPY (Supplemental Figure 4, B and C, and our unpublished results). In addition, *BTN3* overexpression did not affect the growth of yeast-bearing mutations in the COPI components, which principally involved Golgi-ER retrograde sorting (Supplemental Figure 6), nor did it induce Kar2 secretion from the ER. Thus, like Btn2, Btn3 acts upon a specific subset of endosomally sorted proteins at a specific intracellular compartment.

Btn2 localizes to LEs that are labeled by LE/MVB markers such as Vps27 and Snx4 (Kama *et al.*, 2007). Yet Btn3 localizes mainly to the cytoplasm (Figure 3A), unless *BTN2* is up-regulated, as in *btn1*Δ yeast (Pearce *et al.*, 1999), or if it is overexpressed from plasmids, when it also colocalizes with Btn2-labeled compartments (Figures 3A and 4C). Thus Btn2 may facilitate the recruitment of Btn3 from the cytoplasm to endosomal structures. Although the signal for relocalization is unknown, it could be based on the amount of Btn2 available to bind Btn3. However, Btn3 mutants that lack the putative Btn2-interaction domain (i.e., the C terminus of Btn3; Figure 1A) could be recruited to Btn2-labeled compartments (Figure 4C), indicating that other structural features are involved in Btn3 localization. Yet while the Btn3–Btn2 interaction is not essential for Btn3 recruitment, it does appear necessary for the relocalization of Btn2 to large aggregates (Figure 4C; compare rows 2 and 3 with the other rows) that are detergent-insoluble (Figure 4D) and distinct from Ure2- and Hsp104-containing compartments (i.e., the IPOD; Figures 6C and 7B). Thus the Btn3–Btn2 interaction is likely to be important for controlling Btn2 function. This idea is further supported by experiments that reveal that the Snc1 v-SNARE is a competitive inhibitor of the Btn3–Btn2 interaction in vivo and in vitro (Figures 5 and 7C). Therefore the levels of recycling Snc1 at endosomes may interfere with the ability of Btn2 to interact with and/or be sequestered by Btn3. Indeed, *SNC1* overexpression greatly reduced the ability of Btn3 to inhibit Btn2-mediated prion curing (Table 2) and altered the extent of Btn3-Btn2 colocalization (Figure 7C). One might predict then that Btn3 recruitment is requisite only upon certain conditions (e.g., the loss of Btn1 function or conditions when the prion state yields a selective advantage, etc.). However, it does not preclude Btn3 functioning at endosomes under normal growth conditions, since the deletion of *BTN3* improved the retention of overproduced Yif1 at the Golgi (Figure 2A).

Our results suggest that Btn3 regulates Btn2 function by altering Btn2 localization from its site of action (e.g., LEs or sites of Ure2 aggregation; Figures 6C and 7B) and sequestering it in a compartment that is not marked by Ure2 or Hsp104 (Figure 6C, row 3; Figure 7B, rows 3 and 4) and whose nature is not fully known. Although Btn2 localizes to LEs along with retromer components, it does not affect Vps10 and CPY sorting nor colocalize with Vps10-labeled endosomes (Kama *et al.*, 2007), suggesting the existence of multiple endosomal compartments that are serviced by retromer (Kama *et al.*, 2007). Moreover, Wickner et al. (2007) proposed that Btn2 functions in [URE3] prion curing by sequestering aggregated Ure2 at a compartment equivalent to the mammalian aggresome, as it contains other prionogenic substrates like Sup35 or disease-associated Huntingtin aggregates (Kryndushkin *et al.*, 2008). We speculate that this compartment is the IPOD, as Ure2 aggregates mark the IPOD (Kaganovich *et al.*, 2008) and colocalize with Btn2 (Figure 6C; Kryndushkin *et al.*, 2008), and since Btn2 also colocalizes with Hsp104 (Figure 7B), which is known to disaggregate [URE3] prions and enhance their inheritance (Shorter and Lindquist, 2006). This idea is further supported by the finding that Snx4, an endosome marker that colocalizes with Btn2-labeled compartments (Kama *et al.*, 2007), also colocalizes to a large degree with the GFP-VHL IPOD marker in *cim3–1* mutants at 37°C (Supplemental Figure 8B). Btn2 localization to the IPOD may allow for the retrieval of nonaggregated (and functional) proteins to the Golgi and, perhaps, regulate the phenotypic expression of aggregates and/or amyloids (Tyedmers *et al.*, 2010) by targeting them for degradation in the vacuole. This is plausible because both the number and size of Ure2-GFP aggregates in the cells overexpressing *BTN2* were much smaller than those found in WT cells or in cells overexpressing *BTN3*. Although Btn3 does not promote prion curing (Figure 6A; Table 1), it may regulate the sequestration of prion aggregates by down-regulating Btn2 functions, altering Btn2 localization, or both (Figures 2, 4, and 6).

Mechanistically, Snc1 and Btn3 compete for the same binding domain on Btn2 (Figure 5A), and this interplay controls the ability of Btn2 to form productive recycling complexes (i.e., with Snc1) or to be sequestered elsewhere (i.e., with Btn3). How this balance is achieved is unclear but may indicate why a portion of Btn2 is retained in the LE/MVB and/or IPOD, and why GFP-Yif1 is not completely mislocalized to vacuoles upon the overexpression of *BTN3*. A model outlining the roles of Btn2 in both retrograde LE-Golgi trafficking and Ure2 aggregate sequestration, and the consequences of *BTN3* up-regulation are shown (Figure 8). According to this model, Btn2 aids in the retrieval of specific cargo proteins, like Yif1 and Kex2 from the LE (or IPOD), to the Golgi in WT cells and in [URE3]

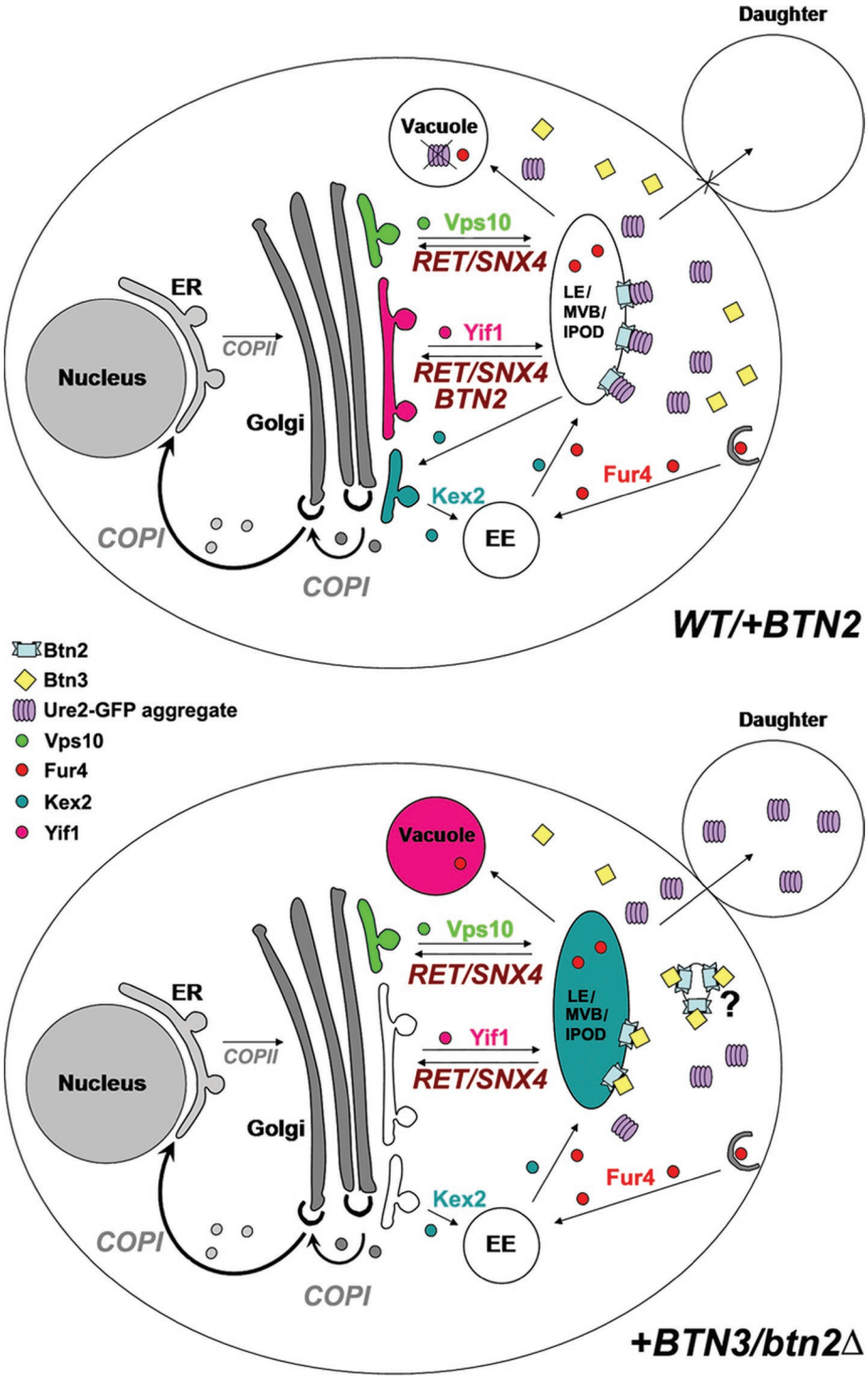

FIGURE 8: A model for Btn3 control of Btn2 function. (Top) WT and *BTN2* up-regulated cells (+*BTN2*): Fur4 (in red) is endocytosed and delivered to early endosomes (EEs) from whence it traffics to a LE/MVB, that may provide access to the IPOD, for either recycling to the PM or delivery to the vacuole for degradation. Yif1 (in pink) exits the Golgi and reaches the LE, where it is retrieved back in a retromer-, Snx4-, and Btn2-dependent manner. Similarly, Kex2 (in turquoise) is trafficked between the *trans*-Golgi and LE via EEs, and is retrieved to the Golgi in a Btn2-dependent manner. In contrast, Vps10 (in light green) is retrieved to the Golgi from the LE/MVB via retromer and Snx4, but in a manner independent of Btn2. Btn3 (in yellow) localizes to the cytoplasm and nucleus, although a portion may colocalize with Btn2 at the LE/MVB/IPOD. Btn2 interacts with Ure2-GFP aggregates/prions (light purple), which normally distribute to daughter cells during cytokinesis. Btn2-mediated sequestration prevents prion distribution to daughters and may target them for degradation in the vacuole. (Bottom) *BTN3* overexpressing cells or *btn2*Δ cells. On *BTN3* overexpression, Btn3 is recruited to the Btn2-labeled LE/MVB/IPOD, where it competes with Snc1 and sequesters Btn2 to a (non-IPOD) compartment (i.e., one not marked by either Ure2 or Hsp104), whereas there is no Btn2 available in *btn2*Δ cells. In either case, the loss of Btn2 availability inhibits Btn2-dependent retrograde transport of specific Golgi proteins and [URE3] prion curing. Thus Yif1 and Kex2 mislocalize to the vacuole and LE, respectively, while the sorting of Vps10 and Fur4 (which is not dependent on Btn2) is unaffected. The loss of Btn2 reduces Ure2 aggregation and degradation and thus facilitates the distribution of [URE3] prion seeds to the daughter cells during cytokinesis.

prion curing upon its overexpression (i.e., reducing the quantity of prion aggregates by sequestration and delivering them to the vacuole for degradation). On the up-regulation of *BTN3*, Btn3 is recruited to endosomes where it competes with Snc1 for binding to Btn2 and sequesters bound Btn2 to another (nonendosomal, non–IPOD, and detergent-insoluble) compartment, whose nature is not yet known. This sequestration reduces the availability of Btn2 to form a recycling complex that confers LE-Golgi retrieval and lowers the level of colocalization between Ure2 and Btn2 to reduce prion curing and therefore increases the concentration of infectious Ure2 aggregates that can be inherited during cytokinesis.

Extensive protein misfolding and aggregation is a common factor that underlies most neurodegenerative diseases (e.g., Alzheimer's, Huntington's, and perhaps Batten disease) and prionogenic disorders. Thus cellular adaptative responses may lessen the impact of these insults by reducing misfolding and aggregation or eliminating the aggregates via storage and/or degradation. Interestingly, *BTN3* encodes a putative oxidoreductase orthologous to *FOXRED1* and may play a role in the cellular response to oxidative stress (Calvo *et al.*, 2010; Fassone *et al.*, 2010). Importantly, we found that *BTN3* overexpression reduces prion curing (Figure 6; Table 1) and increases the number of Ure2-containing particles (Supplemental Figure 9, A and 9B), apart from recruiting endogenously expressed Hsp104 to aggregates under normal conditions of growth (Supplemental Figure 8A). Because induced Hsp104 localizes to the IPOD, along with the Ure2 aggregates (Kaganovich *et al.*, 2008), Btn3 appears to have a direct and positive effect upon [URE3] prion propagation, possibly by sequestering Btn2 and promoting Hsp104 recruitment to the Ure2/IPOD aggregate to promote prion

seed formation. Though the presence of prions is generally thought to be detrimental to cell growth, some have speculated that they might present an adaptive advantage under certain stress conditions (Tyedmers *et al.*, 2008), as opposed to being a consequence of stress. One possibility then is that Btn3 and perhaps its orthologues inhibit protein recycling and prion curing as part of the cellular stress-response mechanism. More work is required to understand this novel family of proteins and to connect oxidoreductase function with endosomal trafficking and prion curing.

MATERIALS AND METHODS

Media, DNA, and genetic manipulation

Yeast were grown on standard rich (YPD) and synthetic complete (SC) media containing either 2% glucose or 3.5% galactose as a carbon source. The preparation of synthetic complete and drop-out media was similar to the method described by Rose *et al.* (1990) (see Haim-Vilmovsky and Gerst, 2009). Adenine-poor medium (0.5× YPD), which contains half the normal amount of yeast extract, was used for the red–white assay for *ADE2* expression. Standard methods were used for the introduction of DNA into yeast and the preparation of yeast genomic DNA (Rose *et al.*, 1990; Haim-Vilmovsky and Gerst, 2009).

Growth tests

For growth tests on plates, yeast were grown to mid–log phase, normalized for optical density at 600 nm (OD_{600}), diluted serially, and plated by drops onto solid medium preincubated at different temperatures. Plates were incubated at the appropriate temperatures for 24–72 h (see figure legends for details).

Two-hybrid assay

The yeast two-hybrid assay was performed as described by Durfee *et al.* (1993), using Btn2 as the bait and a yeast cDNA library as the prey in AH109 cells. Out of ~900,000 transformants, five potential positives were identified, of which one was a true positive and conferred both resistance to the addition of 3AT to the growth medium and β-galactosidase activity on nitrocellulose filters. Assays for cell growth on synthetic medium lacking histidine in the presence of 16 mM 3AT and for β-galactosidase activity on nitrocellulose filters were performed using standard procedures (Durfee *et al.*, 1993). In Figure 1A, yeast (AH109) were transformed with plasmids expressing either the Gal4 DNA-binding domain fused to full-length Btn2 (plasmid pGBK-Btn2; Btn2), the Gal4 transactivating domain fused to full-length Btn3 (plasmid pGAD-$Btn3^{WT}$; Btn3), or both the Gal4 DNA-binding domain fused to full-length Btn2 and various Btn3 deletion mutants fused to the Gal4 transactivating domain (i.e., $Btn3^{1–262}$, plasmid pGAD-$Btn3^{1–262}$; $Btn3^{1–393}$, pGAD-$Btn3^{1–393}$; and $Btn3^{131–523}$, pGAD-$Btn3^{131–523}$). Transformants were grown to mid–log phase in liquid culture prior to serial dilution and plated by drops onto solid medium. For assaying the resistance to 3AT and growth in the absence of histidine, cells were plated onto either control selective medium (SC-LT) or medium lacking histidine and containing 16 mM 3AT (SC-LTH + 3AT). Positive control (+ control) cells expressing p53 (pGBK-p53; Clontech, Mountain View, CA) and SV40 (pGAD-SV40; Clontech) were used in parallel. Cells were grown for 48–60 h at 26°C. In Figure 5A, AH109 yeast cells were transformed with plasmids producing either full-length Btn3 (1–523 aa) or Snc1 lacking its transmembrane domain (3–94 aa) fused to the Gal4 transactivating domain (plasmids pGAD-Btn3 and pGAD-$Snc1^{3–94}$, respectively), and either full-length Btn2 (1–410 aa) or one of its deletion mutants fused to the Gal4 DNA-binding domain (1–100: plasmid pGBK-$Btn2^{1–100}$; 1–213: pGBK-$Btn2^{1–213}$; 1–239: pGBK-$Btn2^{1–239}$; 101–213: pGBK-$Btn2^{101–213}$; 101–239: pGBK-$Btn2^{101–239}$; 101–410: pGBK-$Btn2^{101–410}$; 214–410: pGBK-$Btn2^{214–410}$; and 226–410: pGBK-$Btn2^{226–410}$, respectively). Transformants were grown to mid–log phase in liquid culture prior to serial dilution (×10) and plated by drops and grown, as described above. Positive control (+ control) cells expressing p53 (pGBK-p53) and SV40 (pGAD-SV40), and negative control cells (− control) expressing either full-length pGAD-$Btn3^{WT}$ (left panel) or pGAD-$Snc1^{3–94}$ (right panel) together with a control empty vector (pGBKT7) were used in parallel.

Yeast strains and plasmids

Yeast strains used are listed in Supplemental Table 1. Standard yeast vectors included the following: pRS313 (*CEN HIS3*), pRS316 (*CEN URA3),* pRS426 (2 μm *URA3*), pAD4Δ (2 μm *LEU2 ADH1* promoter), and pAD54 and pAD6 (both are the same as pAD4Δ but contain sequences encoding the HA or myc epitope, respectively, downstream of the *ADH1* promoter). Plasmids used in this study are listed in Supplemental Table 2.

Microscopy

GFP and RFP fluorescence in strains expressing the appropriate GFP- and RFP-tagged fusion proteins was visualized by confocal microscopy (using a Zeiss LSM 710) using cells grown to mid–log phase at 26°C. Representative cells are shown in all figures, although at least 100 cells were examined for each sample and this was done in three independent experiments, except where listed. Endosome and vacuole staining with the vital dye FM4–64 was performed as described by Gabriely *et al.* (2007). For the induction of genes under the control of the *GAL10* promoter (i.e., *URE2-GFP*, *CPY-GFP*, *GAL-BTN2-RFP, GAL-BTN3,* and *GAL-SNC1*), cells were grown in 2% glucose and 2% raffinose-containing media to mid–log phase and then shifted to galactose-containing media until GFP expression was observed.

Immunoprecipitation and Western analysis

Interactions between either HA- or myc-tagged Btn2 and other proteins present in cell lysates were monitored by immunoprecipitation (IP) from cell extracts, as described previously (Kama *et al.*, 2007). IP antibodies included anti-myc antibodies (3 μl per reaction; Santa Cruz Biotechnology, Santa Cruz, CA) and anti-HA antibodies (2.5 μl per reaction; Roche, Indianapolis, IN). Antibodies for protein detection included monoclonal antibodies against the HA epitope (Roche), β-actin (MP Biomedicals, Aurora, OH), GFP (Roche), glutathione *S*-transferase (GST) (Calbiochem, Darmstadt, Germany), His_6 (Sigma-Aldrich, St. Louis, MO) Flag epitope (Sigma-Aldrich), and polyclonal antibodies against maltose-binding protein (NEB, Ipswich, MA) and CPY (Abcam, Cambridge, UK). Samples of total cell lysates (TCLs) (25–30 μg protein per lane) and immunoprecipitates obtained from 500 μg protein of lysate (per IP reaction) were resolved by electrophoresis and detected by Western blotting. Detection was performed by chemiluminescence.

Recombinant protein purification and in vitro binding assay

To perform in vitro binding assays, recombinant His_6-Btn2, GST-Snc1 ($Snc1^{2–94}$), and MBP-Btn3-Flag were generated using the *E. coli* strain BL21-DE3 (genotype: *F^- ompT gal dcm lon hsdS_B(r_B^- m_B^-) χDE3 [lacI lacUV5-T7 gene 1 ind1 sam7 nin5]*) from bacterial expression plasmids and purified using standard procedures. His_6-Btn2 was purified using ProBond resin (Invitrogen, Carlsbad, CA) using a final elution with buffer containing 200 mM imidazole (Kama *et al.*, 2007), and GST-Snc1 was purified using immobilized glutathione

beads (Pierce, Rockford, IL) using a final elution with buffer containing 50 mM glutathione (Kama *et al.*, 2007), while MBP-Btn3-Flag was purified using amylase resin (NEB, Ipswich, MA) using a final elution with buffer containing 10 mM maltose. For competition binding experiments, equal amounts of His_6-Btn2 and MBP-Btn3-Flag (e.g., 3.2×10^{-11} moles) were mixed along with increasing concentrations of GST-tagged Snc1 protein (0–12.8 10^{-11} moles) in binding buffer containing 0.1% NP-40 in phosphate-buffered saline (containing 300 mM NaCl), pH 7.5. Following incubation at 4°C for 12 h, 50 µl of a 50% ProBond slurry prewashed in binding buffer was added, and the samples were incubated with rotation for an additional 2 h at 4°C. Then the samples were washed three times with binding buffer containing 0.1% NP-40 in phosphate-buffered saline (containing 300 mM NaCl) followed by two washes with binding buffer containing 0.1% NP-40 in phosphate-buffered saline (containing 800 mM NaCl), and eluted by the addition of SDS–PAGE sample buffer prior to electrophoresis on 10% SDS–polyacrylamide gels. Proteins were detected quantitatively in blots by using anti-His_6 (1:1000), anti-GST (1:500), and anti-Flag antibodies (1:1000). Stoichiometric determination of Snc1-Btn2 and Btn3-Btn2 binding in vitro was measured by mixing 3.2×10^{-11} moles of His_6-Btn2 with increasing concentrations of either GST-Snc1 or MBP-Btn1-Flag (from 0 to 12.8×10^{-11} moles each) and incubated overnight at 4°C in the same binding buffer, as described above. The protein complexes were pulled down using Probond slurry, resolved by SDS–PAGE, and detected using anti-His_6, anti-GST, and anti-Flag antibodies, as described above. Molar quantification of the proteins precipitated in the binding experiments was determined by electrophoresis and detection (by Western analysis) of known quantities of purified GST-Snc1, His_6-Btn2, and MBP-Btn3-Flag (i.e., 0.2–12.8 $\times$ 10^{-11} moles each) in parallel to the precipitated proteins. Densitometric analysis was used to determine the intensity of the signal arising from a given quantity of purified protein. Linear regressed values were plotted to generate a standard curve to which the densitometric values obtained for the precipitated proteins were plotted and converted into moles of protein precipitated.

Prion curing assay

To quantify [URE3] loss due to the overproduction of Btn2 or Btn3, samples from the whitest colonies from the primary transformation plates were inoculated in liquid YPD at very low density and grown overnight to allow for prion loss. About 500–750 cells were seeded onto 0.5× YPD plates to form colonies. The ratio of red-to-white colonies was scored. Entirely red colonies were scored as arising from cells having lost [*URE3*]. Therefore the percentage of red colonies on the plates is equivalent to the percentage of prion curing. When using plasmids expressing proteins under a galactose-inducible promoter, the same procedure was followed except that the cells were first grown in SC media with 2% raffinose overnight to OD_{600} = 0.5, followed by induction with galactose (3.5% final concentration) for 24–30 h and then plating on 0.5× YPD to suppress further expression from the *GAL* promoter.

Subcellular fractionation and detergent-insoluble protein detection

For the detection of detergent-insoluble proteins, 5 OD_{600} units of mid–log phase grown yeast cells (OD_{600} = 0.5) from each sample were lysed using 0.5-mm glass beads in 300 µl of lysate buffer (1 mM EDTA, 10 mM Tris-HCl, pH 7.5, 150 mM NaCl) devoid of detergent but containing protease inhibitors (e.g., leupeptin, soybean trypsin inhibitor, aprotinin, and pepstatin; each at concentration of 10 µg/ml) and 1 mM phenylmethylsulfonyl fluoride for 45 min. Cell debris was removed by a brief spin at 300 rpm for 2 min. The supernatant (TCL) was then treated with 1% NP-40 (final concentration in the lysis buffer) by addition of 33 µl of 10% NP-40 to the above supernatant followed by a 30-min incubation on ice. The detergent-insoluble pellet (P) fraction was separated from the detergent-soluble (S) fraction by spinning the above lysate at 20,817 $\times$ *g* for 1 h. The pellet fraction was then solubilized in 60 µl of 1× SDS–PAGE sample buffer followed by boiling for 10 min. The distribution of proteins to the detergent-soluble and -insoluble fractions was checked by resolving an equal amount (20 µl) of the supernatant and pellet fractions from each sample on 8% acrylamide gels by SDS–PAGE, followed by Western blotting and detection using the appropriate antibodies.

Immunoblot assay for the detection of intracellular and secreted CPY

Detection of intracellular forms of CPY was carried out as described by Gabriely *et al.* (2007) with minor modifications. Briefly, 5 OD_{600} units of yeast grown to mid–log phase at 26°C were incubated in 500 µl of YPD medium containing 50 mM KPO_4, pH 5.7, for 1 h at 30°C. Then 5 µl of 1 M NaN_3 was added and the cell cultures were cooled on ice for 10 min. Culture samples were centrifuged to separate the cells (containing the intracellular fraction) from the medium. Cell pellets were resuspended in 150 µl of spheroplast-forming buffer (50 mM Tris-HCl, pH 7.4, 1.4 M sorbitol, 2 mM $MgCl_2$, 10 mM NaN_3, freshly added 40 mM β-mercaptoethanol, and 0.15 mg/ml of Zymolase) and incubated with gentle shaking for 30 min at 30°C. Spheroplasts were lysed by the addition of 50 µl of 2% SDS and boiled for 5 min. The lysates were then centrifuged for 10 min at 15,000 $\times$ *g* and the supernatants removed for separation using SDS–PAGE. Samples taken for electrophoresis consisted of an aliquot of 0.5 OD_{600} units (i.e., 20 µl from the above lysate) for the intracellular fraction. SDS sample buffer was added to each sample, and the samples were separated on by SDS–PAGE on 8% acrylamide gels. Following transfer to the nitrocellulose membranes, the blots were incubated with polyclonal anti-CPY antibodies and proteins visualized by enhanced chemiluminescence.

The immunoblot assay for CPY secretion was carried out essentially as described by Gabriely *et al.* (2007), but using the commercial polyclonal anti-CPY antibodies.

Halo assays

Halo assays for measuring the production of biologically active α-factor were performed by spotting *MAT*α yeast strains onto a lawn of *MAT*a *sst2*Δ indicator yeast, as described (Julius *et al.*, 1983). Assays were performed in triplicate.

ACKNOWLEDGMENTS

We thank K. Blumer, O. Deloche, R. Duden, S. Emr, G. Fischer von Mollard, D. Kaganovich, A. Navon, H-D. Schmitt, M. Schuldiner, A. Spang, and R. Wickner for the generous gifts of plasmids and strains. This study was supported by grants to J.E.G. from the Israel Science Foundation (#188/07 and #358/10) and the Irving Harris Foundation, Weizmann Institute, and to both V.K. and J.E.G. from the National Contest for Life (NCL) Foundation, Germany. J.E.G. holds the Besen-Brender Chair in Microbiology and Parasitology, Weizmann Institute.

REFERENCES

Bagola K, Sommer T (2008).Protein quality control: on IPODs and other JUNQ. Curr Biol 18, R1019–R1021.

Brachmann A, Baxa U, Wickner RB (2005). Prion generation in vitro: amyloid of Ure2p is infectious. EMBO J 24, 3082–3092.

Bryant NJ, Stevens TH (1997). Two separate signals act independently to localize a yeast late Golgi membrane protein through a combination of retrieval and retention. J Cell Biol 136, 287–297.
Bugnicourt A, Froissard M, Sereti K, Ulrich HD, Haguenauer-Tsapis R, Galan JM (2004). Antagonistic roles of ESCRT and Vps class C/HOPS complexes in the recycling of yeast membrane proteins. Mol Biol Cell 15, 4203–4214.
Calvo SE *et al*. (2010). High-throughput, pooled sequencing identifies mutations in NUBPL and FOXRED1 in human complex I deficiency. Nat Genet 42, 851–858.
Chattopadhyay S, Muzaffar NE, Sherman F, Pearce DA (2000). The yeast model for batten disease: mutations in BTN1, BTN2, and HSP30 alter pH homeostasis. J Bacteriol 182, 6418–6423.
Chattopadhyay S, Pearce DA (2002). Interaction with Btn2p is required for localization of Rsglp: Btn2p-mediated changes in arginine uptake in Saccharomyces cerevisiae. Eukaryot Cell 1, 606–612.
Chattopadhyay S, Roberts PM, Pearce DA (2003). The yeast model for Batten disease: a role for Btn2p in the trafficking of the Golgi-associated vesicular targeting protein, Yif1p. Biochem Biophys Res Commun 302, 534–538.
Croopnick JB, Choi HC, Mueller DM (1998). The subcellular location of the yeast Saccharomyces cerevisiae homologue of the protein defective in the juvenile form of Batten disease. Biochem Biophys Res Commun 250, 335–341.
Dilcher M, Kohler B, von Mollard GF (2001). Genetic interactions with the yeast Q-SNARE VTI1 reveal novel functions for the R-SNARE YKT6. J Biol Chem 276, 34537–34544.
Duden R, Hosobuchi M, Hamamoto S, Winey M, Byers B, Schekman R (1994). Yeast beta- and beta'-coat proteins (COP). Two coatomer subunits essential for endoplasmic reticulum-to-Golgi protein traffic. J Biol Chem 269, 24486–24495.
Durfee T, Becherer K, Chen PL, Yeh SH, Yang Y, Kilburn AE, Lee WH, Elledge SJ (1993). The retinoblastoma protein associates with the protein phosphatase type 1 catalytic subunit. Genes Dev 7, 555–569.
Fassone E *et al*. (2010). FOXRED1, encoding an FAD-dependent oxidoreductase complex-I-specific molecular chaperone, is mutated in infantile-onset mitochondrial encephalopathy. Hum Mol Genet 19, 4837–4847.
Fischer von Mollard G, Nothwehr SF, Stevens TH (1997). The yeast v-SNARE Vti1p mediates two vesicle transport pathways through interactions with the t-SNAREs Sed5p and Pep12p. J Cell Biol 137, 1511–1524.
Fischer von Mollard G, Stevens TH (1999). The Saccharomyces cerevisiae v-SNARE Vti1p is required for multiple membrane transport pathways to the vacuole. Mol Biol Cell 10, 1719–1732.
Franzusoff A, Redding K, Crosby J, Fuller RS, Schekman R (1991). Localization of components involved in protein transport and processing through the yeast Golgi apparatus. J Cell Biol 112, 27–37.
Fuller RS, Brake A, Thorner J (1989). Yeast prohormone processing enzyme (KEX2 gene product) is a Ca2+-dependent serine protease. Proc Natl Acad Sci USA 86, 1434–1438.
Gabriely G, Kama R, Gerst JE (2007). Involvement of specific COPI subunits in protein sorting from the late endosome to the vacuole in yeast. Mol Cell Biol 27, 526–540.
Getty AL, Pearce DA (2011). Interactions of the proteins of neuronal ceroid lipofuscinosis: clues to function. Cell Mol Life Sci 68, 453–474.
Gurunathan S, Chapman-Shimshoni D, Trajkovic S, Gerst JE (2000). Yeast exocytic v-SNAREs confer endocytosis. Mol Biol Cell 11, 3629–3643.
Haim-Vilmovsky L, Gerst JE (2009). m-TAG: a PCR-based genomic integration method to visualize the localization of specific endogenous mRNAs in vivo in yeast. Nat Protoc 4, 1274–1284.
Haskell RE, Carr CJ, Pearce DA, Bennett MJ, Davidson BL (2000). Batten disease: evaluation of CLN3 mutations on protein localization and function. Hum Mol Genet 9, 735–744.
Hettema EH, Lewis MJ, Black MW, Pelham HR (2003). Retromer and the sorting nexins Snx4/41/42 mediate distinct retrieval pathways from yeast endosomes. EMBO J 22, 548–557.
Ito T, Chiba T, Ozawa R, Yoshida M, Hattori M, Sakaki Y (2001). A comprehensive two-hybrid analysis to explore the yeast protein interactome. Proc Natl Acad Sci USA 98, 4569–4574.
Jarvela I, Lehtovirta M, Tikkanen R, Kyttala A, Jalanko A (1999). Defective intracellular transport of CLN3 is the molecular basis of Batten disease (JNCL). Hum Mol Genet 8, 1091–1098.
Jarvela I, Sainio M, Rantamaki T, Olkkonen VM, Carpen O, Peltonen L, Jalanko A (1998). Biosynthesis and intracellular targeting of the CLN3 protein defective in Batten disease. Hum Mol Genet 7, 85–90.
Johnson PE, Donaldson LW (2006). RNA recognition by the Vts1p SAM domain. Nat Struct Mol Biol 13, 177–178.
Julius D, Blair L, Brake A, Sprague G, Thorner J (1983). Yeast alpha factor is processed from a larger precursor polypeptide: the essential role of a membrane-bound dipeptidyl aminopeptidase. Cell 32, 839–852.
Kaganovich D, Kopito R, Frydman J (2008). Misfolded proteins partition between two distinct quality control compartments. Nature 454, 1088–1095.
Kama R, Robinson M, Gerst JE (2007). Btn2, a Hook1 ortholog and potential Batten disease-related protein, mediates late endosome-Golgi protein sorting in yeast. Mol Cell Biol 27, 605–621.
Katz ML, Gao CL, Prabhakaram M, Shibuya H, Liu PC, Johnson GS (1997). Immunochemical localization of the Batten disease (CLN3) protein in retina. Invest Ophthalmol Vis Sci 38, 2375–2386.
Kim Y, Chattopadhyay S, Locke S, Pearce DA (2005). Interaction among Btn1p, Btn2p, and Ist2p reveals potential interplay among the vacuole, amino acid levels, and ion homeostasis in the yeast Saccharomyces cerevisiae. Eukaryot Cell 4, 281–288.
Kramer H, Phistry M (1996). Mutations in the Drosophila hook gene inhibit endocytosis of the boss transmembrane ligand into multivesicular bodies. J Cell Biol 133, 1205–1215.
Kremmidiotis G, Lensink IL, Bilton RL, Woollatt E, Chataway TK, Sutherland GR, Callen DF (1999). The Batten disease gene product (CLN3p) is a Golgi integral membrane protein. Hum Mol Genet 8, 523–531.
Kryndushkin DS, Shewmaker F, Wickner RB (2008). Curing of the [URE3] prion by Btn2p, a Batten disease-related protein. EMBO J 27, 2725–2735.
Kyttala A, Lahtinen U, Braulke T, Hofmann SL (2006). Functional biology of the neuronal ceroid lipofuscinoses (NCL) proteins. Biochim Biophys Acta 1762, 920–933.
Lee CH *et al*. (2010). Involvement of Vts1, a structure-specific RNA-binding protein, in Okazaki fragment processing in yeast. Nucleic Acids Res 38, 1583–1595.
Lewis MJ, Nichols BJ, Prescianotto-Baschong C, Riezman H, Pelham HR (2000). Specific retrieval of the exocytic SNARE Snc1p from early yeast endosomes. Mol Biol Cell 11, 23–38.
Lustgarten V, Gerst JE (1999). Yeast VSM1 encodes a v-SNARE binding protein that may act as a negative regulator of constitutive exocytosis. Mol Cell Biol 19, 4480–4494.
Marash M, Gerst JE (2003). Phosphorylation of the autoinhibitory domain of the Sso t-SNAREs promotes binding of the Vsm1 SNARE regulator in yeast. Mol Biol Cell 14, 3114–3125.
Matern H, Yang X, Andrulis E, Sternglanz R, Trepte HH, Gallwitz D (2000). A novel Golgi membrane protein is part of a GTPase-binding protein complex involved in vesicle targeting. EMBO J 19, 4485–4492.
Mole SE, Williams RE, Goebel HH (2005). Correlations between genotype, ultrastructural morphology and clinical phenotype in the neuronal ceroid lipofuscinoses. Neurogenetics 6, 107–126.
Mosser DD, Ho S, Glover JR (2004). Saccharomyces cerevisiae Hsp104 enhances the chaperone capacity of human cells and inhibits heat stress-induced proapoptotic signaling. Biochemistry 43, 8107–8115.
Oberstrass FC, Lee A, Stefl R, Janis M, Chanfreau G, Allain FH (2006). Shape-specific recognition in the structure of the Vts1p SAM domain with RNA. Nat Struct Mol Biol 13, 160–167.
Oh JJ, Grosshans DR, Wong SG, Slamon DJ (1999). Identification of differentially expressed genes associated with HER-2/neu overexpression in human breast cancer cells. Nucleic Acids Res 27, 4008–4017.
Pearce DA, Ferea T, Nosel SA, Das B, Sherman F (1999). Action of BTN1, the yeast orthologue of the gene mutated in Batten disease. Nat Genet 22, 55–58.
Pearce DA, Sherman F (1997). BTN1, a yeast gene corresponding to the human gene responsible for Batten's disease, is not essential for viability, mitochondrial function, or degradation of mitochondrial ATP synthase. Yeast 13, 691–697.
Persaud-Sawin DA, McNamara JO, 2nd, Rylova S, Vandongen A, Boustany RM (2004). A galactosylceramide binding domain is involved in trafficking of CLN3 from Golgi to rafts via recycling endosomes. Pediatr Res 56, 449–463.
Poirot O, O'Toole E, Notredame C (2003). Tcoffee@igs: A web server for computing, evaluating and combining multiple sequence alignments. Nucleic Acids Res 31, 3503–3506.
Protopopov V, Govindan B, Novick P, Gerst JE (1993). Homologs of the synaptobrevin/VAMP family of synaptic vesicle proteins function on the late secretory pathway in S. cerevisiae. Cell 74, 855–861.

Rakheja D, Narayan SB, Bennett MJ (2008). The function of CLN3P, the Batten disease protein. Mol Genet Metab 93, 269–274.
Richardson SC, Winistorfer SC, Poupon V, Luzio JP, Piper RC (2004). Mammalian late vacuole protein sorting orthologues participate in early endosomal fusion and interact with the cytoskeleton. Mol Biol Cell 15, 1197–1210.
Robinson M, Poon PP, Schindler C, Murray LE, Kama R, Gabriely G, Singer RA, Spang A, Johnston GC, Gerst JE (2006). The Gcs1 Arf-GAP mediates Snc1,2 v-SNARE retrieval to the Golgi in yeast. Mol Biol Cell 17, 1845–1858.
Rose MD, Winston F, Hieter P (1990). Methods in Molecular genetics: A Laboratory Course Manual, New York, NY: Cold Spring Harbor Laboratory Press.
Schaupp A, Marcinowski M, Grimminger V, Bosl B, Walter S (2007). Processing of proteins by the molecular chaperone Hsp104. J Mol Biol 370, 674–686.
Seaman MN (2005). Recycle your receptors with retromer. Trends Cell Biol 15, 68–75.
Seaman MN (2008). Endosome protein sorting: motifs and machinery. Cell Mol Life Sci 65, 2842–2858.
Shorter J, Lindquist S (2006). Destruction or potentiation of different prions catalyzed by similar Hsp104 remodeling activities. Mol Cell 23, 425–438.
Stefan CJ, Blumer KJ (1999). A syntaxin homolog encoded by VAM3 mediates down-regulation of a yeast G protein-coupled receptor. J Biol Chem 274, 1835–1841.
Stein IS, Gottfried A, Zimmermann J, Fischer von Mollard G (2009). TVP23 interacts genetically with the yeast SNARE VTI1 and functions in retrograde transport from the early endosome to the late Golgi. Biochem J 419, 229–236.
Sunio A, Metcalf AB, Kramer H (1999). Genetic dissection of endocytic trafficking in Drosophila using a horseradish peroxidase-bride of sevenless chimera: hook is required for normal maturation of multivesicular endosomes. Mol Biol Cell 10, 847–859.
Tyedmers J, Madariaga ML, Lindquist S (2008). Prion switching in response to environmental stress. PLoS Biol 6, e294.
Tyedmers J, Treusch S, Dong J, McCaffery JM, Bevis B, Lindquist S (2010). Prion induction involves an ancient system for the sequestration of aggregated proteins and heritable changes in prion fragmentation. Proc Natl Acad Sci USA 107, 8633–8638.
Walenta JH, Didier AJ, Liu X, Kramer H (2001). The Golgi-associated hook3 protein is a member of a novel family of microtubule-binding proteins. J Cell Biol 152, 923–934.
Wickner RB, Edskes HK, Shewmaker F, Nakayashiki T, Engel A, McCann L, Kryndushkin D (2007). Yeast prions: evolution of the prion concept. Prion 1, 94–100.
Wilcox CA, Fuller RS (1991). Posttranslational processing of the prohormone-cleaving Kex2 protease in the Saccharomyces cerevisiae secretory pathway. J Cell Biol 115, 297–307.